

SOLAR EVAPORATION OF
SALINE WATER UNDER VACUUM

by

Esber Ibrahim Shaheen

A Thesis Submitted to the Faculty of the
DEPARTMENT OF CHEMICAL ENGINEERING
In Partial Fulfillment of the Requirements
For the Degree of
MASTER OF SCIENCE
In the Graduate College
THE UNIVERSITY OF ARIZONA

1 9 6 4

STATEMENT BY AUTHOR

This thesis has been submitted in partial fulfillment of requirements for an advanced degree at The University of Arizona and is deposited in The University Library to be made available to borrowers under rules of the Library.

Brief quotations from this thesis are allowable without special permission, provided that accurate acknowledgement of source is made. Requests for permission for extended quotation from or reproduction of this manuscript in whole or in part may be granted by the head of the major department or the Dean of the Graduate College when in their judgment the proposed use of the material is in the interests of scholarship. In all other instances, however, permission must be obtained from the author.

SIGNED: Esher J. Shaheen

APPROVAL BY THESIS DIRECTOR

This thesis has been approved on the date shown below:



D. H. WHITE, Head
Department of Chemical Engineering

5/10/64
Date

TABLE OF CONTENTS

	<u>PAGE</u>
LIST OF ILLUSTRATIONS	iv
LIST OF TABLES	vii
ABSTRACT	viii
I. INTRODUCTION	1
II. OBJECTIVE	4
III. SURVEY OF LITERATURE	6
A. Solar Distillers using collectors with optical concentration of solar energy.	10
B. Stationary solar distillers, or distillers without solar energy concentrating devices.	12
IV. PROPOSED SOLAR EVAPORATION PROCESS FOR SALINE WATER IN ARID REGIONS	31
A. Description of Process.	31
B. General Calculations and Assumptions.	33
C. Calculated Cases.	41
V. DESCRIPTION OF APPARATUS	48
A. Evaporator	51
B. Condenser	53
C. Pumps	53
D. Feed Column	55
E. Air Blower	55
F. Electric System	55

TABLE OF CONTENTS
(Continued)

	<u>PAGE</u>
G. Thermocouples	56
H. Air-Meter	58
I. Epply Radiation Pyrheliometer	60
J. Flow System	60
VI. PROCEDURE	62
A. Calibrations	62
B. Air Leak Prevention	64
C. Plexiglas Transmission and Incident Radiation	65
D. Operation	66
VII. PRESENTATION OF EXPERIMENTAL DATA	68
VIII. DISCUSSION OF RESULTS	73
A. Heat and Mass Balances	73
B. Analysis of Results	83
IX. SUMMARY	93
X. RECOMMENDATIONS	95
XI. ACKNOWLEDGEMENTS	97
XII. LITERATURE CITED	98
XIII. APPENDIX	102
A. Data from Test Runs	103
B. General Approach for Heat and Mass Balance Around a Regular Deep- Basin Solar Still.	110
C. Nomenclature	116

LIST OF ILLUSTRATIONS

<u>FIGURE</u>	<u>PAGE</u>
1. Schematic Flow Diagram of a Standard Greenhouse-type Solar Still.	13
2. Inflatable Type Solar Distiller.	19
3. Schematic Cross Section of a Flat Tilted Solar Still.	21
4. Diagram of a Multiple-Effect Solar Still.	23
5. Approximate Schematic Flow Diagram for a Humidification Process.	25
6. Schematic Diagram of a Portable Solar Still.	27
7. Flow Diagram for a Vacuum Desalinator of Solar Heater Type.	29
8. Schematic Flow Diagram for the Proposed Process.	32
9. Schematic Flow Diagram of Experimental Process.	49

LIST OF ILLUSTRATIONS
(Continued)

<u>FIGURE</u>		<u>PAGE</u>
10.	Photograph of Apparatus.	50
11.	Sketch of the Inner Cylinder (Evaporator).	52
12.	Sketch of the Outer Cylinder Section.	54
13.	Photograph of the Infrared Lamp and its Reflector.	57
14.	Distribution of Thermocouples Around the Evaporator.	59
15.	Thermocouple Calibration for Thermocouple Number 0.	63
16.	Heat Available for Water Evaporation Versus Pressure Applied Inside the Evaporator.	84
17.	Rate of Heat Loss by Conduction Through the Walls as a Function of the Pressure Inside the Evaporator.	85
18.	Rate of Water Collected from the Condenser Chamber as a Function of the Applied Pressure Inside the Evaporator.	88

LIST OF ILLUSTRATIONS
(Continued)

<u>FIGURE</u>		<u>PAGE</u>
19.	Water Basin Temperature as a Function of the Pressure Applied Inside the Evaporator.	89
20.	Average Wall Temperature of the Evaporator as a Function of the Pressure Inside the Evaporator.	91
21.	Temperature of the Underside of the Plexiglas Cover Versus the Pressure Inside the Evaporator.	92

LIST OF TABLES

<u>TABLE</u>		<u>PAGE</u>
I.	Approximate Distribution of Solar Radiation Reaching Deep-Basin Still (Based on a 3-day energy balance run in October).	17
II.	Estimation of the Average Glass Cover Temperature for the Proposed Process.	43
III.	Pressure Inside the Evaporator for each Run, and Basin Water Temperature at Steady-State.	70
IV.	Heat Available for Water Evaporation in the Respective Runs.	70
V.	Actual Heat Distribution for the Respective Runs.	71
VI.	Percentage Distribution of the Incident Radiation.	72
VII.	Data From Test Runs at Steady-State.	103
VIII.	Data From Run Number 3.	106

ABSTRACT

The basic objective of this research was the desalination of sea or brackish water using solar energy and vacuum techniques. A process using the vacuum technique was devised for the desalination of sea or brackish water under desert conditions, and calculations were made to show the advantages of this process. To simulate a section of this overall process, an evaporator which may be operated at pressures ranging from relatively low vacuum to one atmosphere was designed. This evaporator was used to convert saline water into fresh water. Solar energy was simulated by using artificial lamps for the conversion process, and fresh water was used experimentally in place of saline water. The purpose was to obtain data on the relationship between the applied vacuum inside the evaporator, the fresh water yield, and the heat distribution in the system.

The evaporator consisted of a hollow cylinder made of K-Monel with the bottom made of the same metal and painted

black on the inside. Radiant energy from an infrared artificial lamp was transmitted through clear methyl-methacrylate (Plexiglas) which was fitted on the top of the cylinder. The vapor was drawn to a coil and shell condenser where it was condensed and collected. The vacuum applied on the system was controlled manually.

Six runs were made with a constant batch feed of water, and each run was continued until the system reached a steady-state.

A heat balance was made for each run, and the amount of heat available for water evaporation was compared to the weight of water evaporated and collected in the condenser chamber. Due to the application of vacuum and due to the absorptivity of the Plexiglas top, radiation always occurred from the Plexiglas top to the water basin

The fresh water yield increased with a decrease in the pressure applied inside the evaporator. For a pressure of 0.46 lb/in^2 inside the evaporator, the rate of fresh water production was 72 g/hr while for a pressure of 1.28 lb/in^2 inside the evaporator, the rate of water

production was 55 g/hr. The heat available for evaporation increased with a decrease in the pressure applied on the system. When the applied pressure was 5 lb/in², 37.4 per cent of the incident radiation was available for water production; and when the pressure decreased to 0.46 lb/in² the heat available for water evaporation was 52.6 per cent of the incident radiation.

This investigation revealed the applicability of using vacuum techniques in saline water conversion. Recommended further research consisted mainly of investigating the productivity of the still when it is used under the sun in a desert site. Once these investigations are accomplished a main application of this process may be to furnish municipal water to communities. It may be also possible to develop a household desalting unit which could compete economically with the best household desalting units on the market today.

I. INTRODUCTION

Water is a vital ingredient of life. A growing demand for fresh water as communities and industry grow and new industry develops has produced shortages in many areas around the world. For this reason, there is much interest today in the problem of converting sea water to fresh water. Since the cost of energy plays a decisive role in distillation processes, it is attractive to attempt to harness the power from the sun for this purpose. One major disadvantage of solar energy use in saline water conversion is the low production rate attributed to solar stills. This research was directed toward the development of a process which would directly contribute to the increase in fresh water yield by decreasing radiant and convective heat losses, and would contribute, indirectly, to the lowering of the costs of saline water conversion.

The process of solar evaporation of saline water under vacuum was chosen. The background leading to this

selection was that in 1961, D. H. White originated the basic idea of desert evaporation under vacuum, utilizing cooling tower water to achieve the lower temperature necessary to condense the evaporator vapors. The work on this process was initiated in the summer of 1962 under the direction of D. H. White.

The effects of operating pressure and applied wattage on the fresh water yield, and the operational characteristics, reliability and faults of the newly-designed apparatus were investigated. Calculations were made for the purpose of presenting the heat distribution in the experimental research and helping in the design of a process for saline water conversion in arid regions. Solar energy was simulated by using artificial lamps, and distilled water, instead of saline water, was used in this research. Sea water concentration is usually three and a half per cent in salts, and if sea water is concentrated to seven per cent salt content the boiling point elevation is 1.2 °F (1). If sea water were used in this research, the salt concentration in the unevaporated water would not exceed seven per cent due to the considerably small amount of water evaporated. Thus, the influence of the boiling point

elevation on the net results of the research is negligible.

II. OBJECTIVE

The primary objective of this research was to provide information pertinent to the development and design of an economical process for saline water conversion in arid regions. The process of interest consisted of saline water conversion using vacuum, solar energy, and the low temperatures in a cooling tower. The application of vacuum decreased the boiling point of water and, thus, decreased radiation and convection losses to the atmosphere. A cooling tower would provide low temperature cooling water for water vapor condensation under vacuum.

The data pertinent to the development of the process were sought from two directions of investigation;

1. Calculations for the experimental equipment and for some arid region cases. The purpose of the calculations for the arid region cases was to demonstrate the superiority of this process compared with other processes using solar energy for saline water conversion.

2. Experimental research simulating a section of the process and demonstrating the advantages of vacuum application.

III. SURVEY OF LITERATURE

Salt water oceans occupy nearly three-quarters of the earth's surface, and sixty per cent of the remaining quarter is arid land (29*). In these arid lands, the dry season may last for several months, during which the energy of the sun is abundant and represents a potentially large fuel resource. Thus, much interest has materialized in the problem of converting sea water to fresh water using solar energy. This interest stems from the growing realization of the possibility of acute shortages of naturally available potable water. Industrial growth in some normally semi-arid regions has contributed to the urgency of this situation. Moreover, the economical conversion of sea water or saline water into fresh water may open for use large areas of the above-mentioned arid lands.

The United States of America has taken a special interest in saline water conversion research. The original

* Numbers in parentheses refer to Literature cited.

concept of the saline water program included major effort in stimulating private scientific interest and activity in development of processes. A special department called The Office of Saline Water (OSW) was established within the United States Department of the Interior. A large number of research projects were carried out under the sponsorship of the Office of Saline Water. The better processes were then further developed by building various demonstration plants of large capacities to test the suitability of each type of plant in operation and to explore their economic aspects. The following projects have been adopted by the Office of Saline Water (12);

1. A sea water conversion solar research station was established at Daytona Beach, Florida. A deep-basin, glass-covered solar still was used covering an area of 2500 square feet with an average fresh water production of five hundred gallons per day.
2. In Freeport, Texas, a plant with a capacity of one million gallons per day was built using the long-tube vertical multiple-effect evaporation process.
3. In San Diego, California, the multistage-

flash distillation process was used, and the plant was built with a capacity of one million gallons per day.

4. In Roswell, New Mexico, a plant using the process of forced circulation vapor-compression was built with a capacity of one million gallons per day.
5. In Wrightsville Beach, North Carolina, a freezing process was used, and the plant was built with a capacity of two hundred and fifty thousand gallons per day.
6. In Webster, South Dakota, a plant using the process of electrodialysis (membrane process) was built with a fresh water production rate of two hundred and fifty thousand gallons per day.

Around the world, the saline water conversion research has been most active in the European countries. The Organization for European Economic Cooperation (O.E.E.C.), which is an organization founded by the free European countries, created Group Number Eight for the study of methods for desalting sea and brackish waters and for

coordinating the research in the following countries: Belgium, Denmark, France, Germany, Great Britain, Holland, and Sweden. The Soviet Union is doing extensive research in saline water conversion, but the United States is by far the most active country of the world in the saline water conversion research.

Of the various methods of desalination, the one that has been in use the longest is solar distillation. This method may perform an important function in supplying fresh water to areas rich in sunshine and relatively poor in fuel (21).

Solar distillers can be divided into two groups depending on the type of collector used. The collector is that part of the solar still which accumulates the solar energy in order to raise the temperature of the salt water contained in the collector. Collectors are classified into two groups, those with optical concentration of solar energy such as lenses or reflectors, and those without optical concentration of solar energy. The latter are usually stationary installations which receive solar energy directly (2, 8, 11, 35).

A. Solar distillers using collectors with optical concentration of solar energy

Lenses, as concentrating devices for solar energy, can be used in very small units. In all other cases, various kinds of mirrors and mirror assemblies are used. Parabolic reflectors were used centuries ago to concentrate solar energy to a boiler. The vapor produced was condensed by conventional means (2, 11, 35). In 1770, Lavoisier, the French scientist, concentrated solar rays by using a large lens supported in an elaborate mounting.

Abbot's solar distiller consisted of a cylindrical parabolic reflector. The surface of the reflector was made of aluminum foil. Solar rays were concentrated to a vacuum-jacketed tube located at the focus of the parabolic mirror. The reflector, intercepting 11 square feet of solar radiation, was used in Florida in 1938, producing two to three gallons of fresh water per day (11, 35). This solar distiller typifies in weight and construction most of the concentrating devices. In general, a reliable moving mechanism is attached to such devices to permit the concentrator to follow the sun. This is done within close limits to permit keeping the boiler in the focus of the concentrating

device. Back-silvered glass reflectors or polished and anodized aluminum reflectors may concentrate 80 to 90 per cent of the direct part of the incident solar radiation.

Cost estimates have indicated that none of the concentrating devices could produce water at a cost lower than \$3.25 per 1000 gallons of fresh water (2). It has been stated that additional research could decrease this cost figure to \$2.20 per 1000 gallons of water. According to these cost figures, it appears that concentrating devices are not the answer to the water problem. The major problems faced in solar energy concentrating stills are:

(a) Only the direct part of the solar beam can be concentrated and the diffuse solar energy represents a loss which is as high as ten per cent of the total energy on clear days and appreciably higher on cloudy days. This loss is an inherent disadvantage of this type of solar still.

(b) Precise movement of the reflectors is required to permit the coincidence of the image formation and the boiler. The continuous requirement of this movement, even in high winds, complicates the design and contributes to increasing the water production cost.

(c) Single-effect stills operating with concentrating devices could not be economical due to the high cost of equipment and labor. Multiple-effect stills require a complication of design which raises the cost of water production.

Collecting and concentrating solar energy is receiving a limited treatment in this survey, because concentrating devices have proved too expensive for salt water purification (2). For this reason, more attention is given to solar distillers without solar energy concentrating devices.

B. Stationary solar distillers, or distillers without solar energy concentrating devices

Numerous devices of this type have been reviewed in a Symposium on Saline Water Conversion (1957), publication 568, Office of Saline Water, U. S. Department of the Interior (ref. 21, pp. 117-176). The types which seem to be economically promising are as follows:

1. Greenhouse-type-simple solar still. A shallow basin, painted black to absorb the rays of the sun, is filled with saline water (see Figure 1). Heat from the sun is transmitted through a transparent inclined cover and

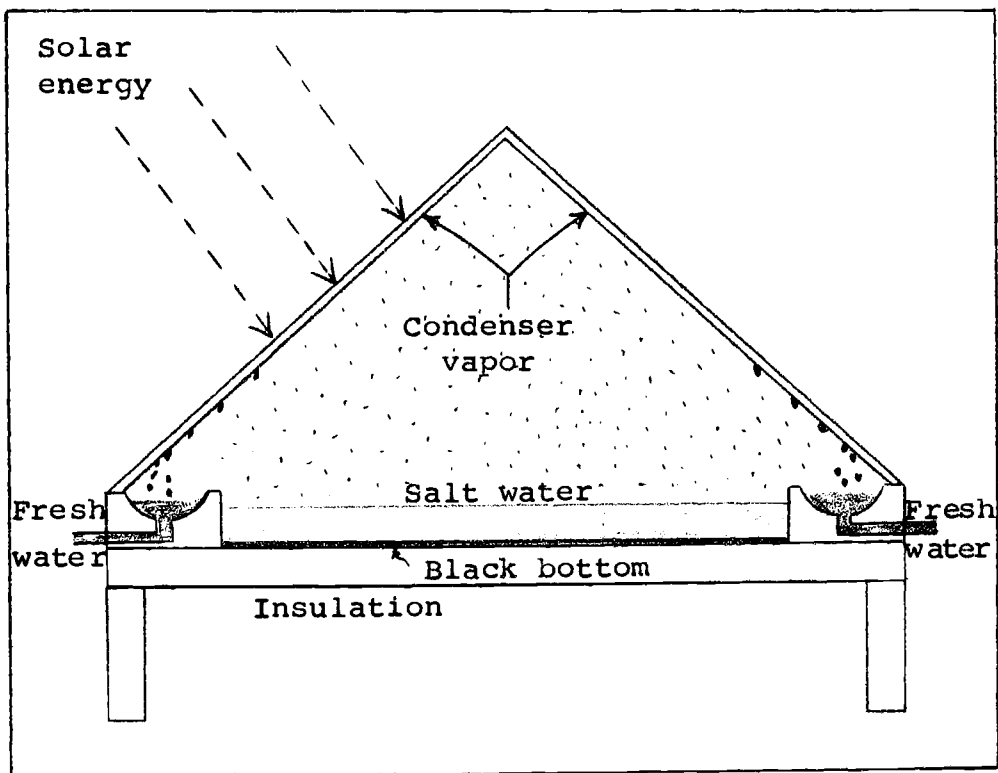


Figure 1: Schematic Flow Diagram of a Standard Greenhouse-type Solar Still.

causes the water to evaporate. The saturated vapor inside the still condenses on the inside of the transparent surface, owing to the lower temperature of the transparent surface compared with the water basin temperature. When the inner surface of the transparent medium is clean, the condensed droplets move along the inclination owing to the adhesion between the water and the transparent surface. The condensate flows into collecting troughs placed on each side of the still (1, 2, 8, 13, 21, 25, 26, 27, 30, 31, 33, 35). In such a still, water does not boil but vaporizes slowly and the vapors reach the cooler surface by convection.

The largest and oldest solar distillation still of this type was built in 1872 by Charles Wilson, near the harbor of Antofagasta at Las Salinas in Chile (35). The brine feed contained 14 per cent salts and was pumped from nearby wells. Water basins were made of black painted wood. The total occupied area was 51000 square feet, and the highest water yield was 6000 gallons per day or approximately one pound of fresh water per day per square foot of horizontal area. On hot days, the maximum temperature of the water in the basin was 150°F, and the surrounding air temp-

erature was 80°F, around noon. The total cost of the installation including all accessories was \$250,000 (2). The efficiency of this still was about 35 per cent, and it operated up to 1908, with 36 years of operation to prove the durability of glass (11).

A roof-type solar still was designed by Dr. Maria Telkes, and it was operated during the summer of 1951. The tray rested on an insulating support. The base area was 200 square feet with a maximum daily production of 1.2 pounds of fresh water per square foot (2).

Today, there are two major greenhouse-type solar stills:

(a) Plastic-covered stills. The basins of the plastic-covered stills are maintained relatively shallow in water depth. Insulation is provided under the water-tight basins. Covers of the stills are made of plastic materials instead of glass. The covers are supported by a slight pressure of air supplied from a small fan. Except for concrete curbs, the basin is also constructed of plastic materials. Plastic stills were built by E. I. duPont de Nemours and Company. Small stills were covered by du Pont polyvinyl fluoride Teslar film, and larger stills had a

cover of Polyethylene teraphthalate Mylar film (1, 2).

(b) "Deep Basin" glass-covered stills consist of basins which are constructed on level ground and are covered by glass plates. This type of still was designed originally by Dr. Löf, (21, 25, 26) who modified the design of the simple solar still. The large single basin is subdivided into smaller basins by means of curbing which serve as glass supports. The glass plates make an angle of 15 degrees with the bottom of the basin for the purpose of having better solar reception and to minimize the amount of air circulating inside the still. The main principle of the "Deep Basin" still is to make use of the heat storage capacity of the water in the basin to provide continuous distillation even during the night. In the experimental process, the basin is placed directly on the ground and insulation is used only for the side walls. The water level in the basin may be as high as one foot. A heat exchanger is used to preheat the sea water feed by the leaving condensate and the residue streams (1). The average monthly efficiencies for this kind of still varied between 26 to 35 per cent based on the mean values of solar radiation and atmospheric temperature for each day. The energy

distribution in a Deep-Basin still is best described by the following table taken from Reference (1), page 171:

TABLE I

Approximate Distribution of Solar Radiation Reaching Deep-Basin Still (Based on 3-day energy balance run in October, 1959).

Distribution	% of Solar Radiation ^a
Evaporation	32
Brine leakage and vapor loss	0
Ground and edge heat loss	2
Solar radiation absorbed by cover	10
Solar radiation reflected by still	12
Radiation from water in basin	25
Internal convection	7
Re-evaporation of distillate and unaccounted-for losses	<u>12</u>
Total	100

^aIncident solar radiation averaged 1400 Btu/sq.ft./day over a 3-day period.

2. Inflatable, floating solar distiller. During World War II, flyers forced down at sea were equipped with inflatable rubber life rafts, but these life rafts could carry only a limited amount of fresh water. Thus, the need for a floating solar distiller developed, since most flying was over oceans in tropical regions where solar energy is most available (see Figure 2). The floating solar still is made of Vinylite (polyvinyl chloride acetate) or similar plastic materials (11). A black porous pad is saturated with sea water and supported by the inflatable envelope. The plastic envelope transmits solar rays, which, in turn, heats the sea water in the black pad. The resulting vapor condenses and trickles along the envelope inclination. Fresh water is received in a water-collecting chamber situated at the bottom of the elliptic-shaped plastic envelope. A plug attached to the water-collecting chamber permits fresh water withdrawal when needed. At the end of the day, the salt in the black pad is flushed out, and the process might be repeated over and over every day. The maximum temperature reached by the black pad is 150°F, and the still efficiency ranged from 50 to 60 per cent.

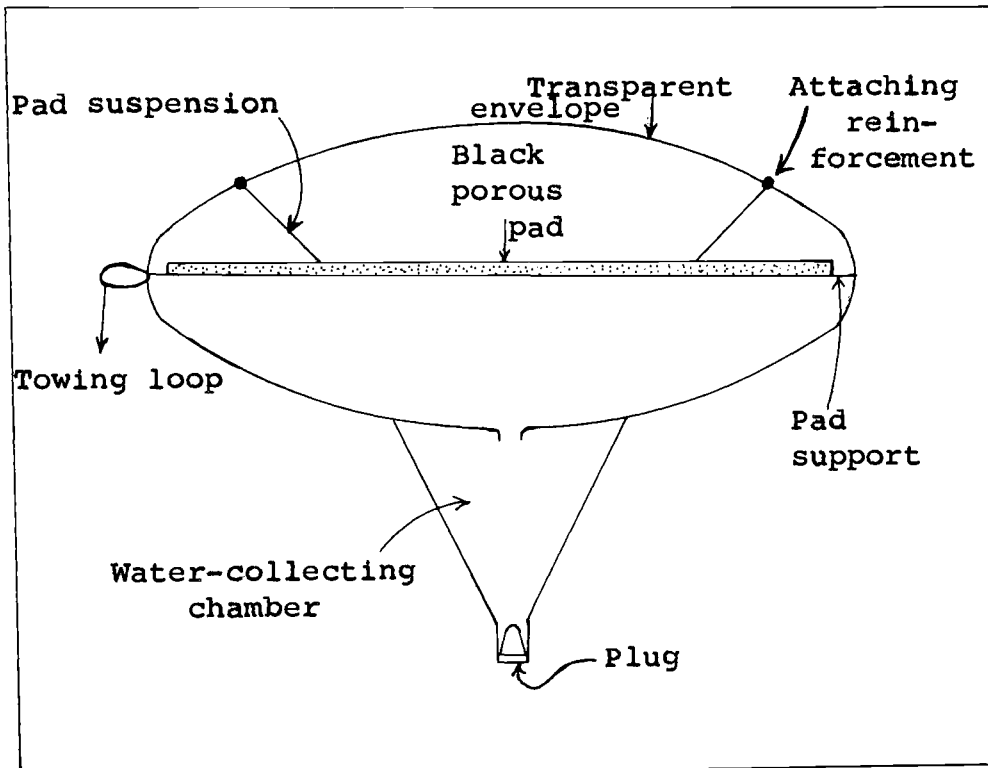


Figure 2: Inflatable Type Solar Distiller.

3. Single-effect flat tilted solar still. At various latitudes, the energy reception by a tilted surface is higher than that received by a horizontal surface. At latitude 35 degrees, fixed tilting could increase the annual solar energy received over a horizontal surface by 24 per cent. This consideration resulted in a new solar still design by Dr. Telkes (see Figure 3). Saline water is fed to a porous pad, instead of a horizontal tray. A supporting wooden frame is covered on its top by a transparent glass surface. It is essential to avoid dropwise condensation, since droplets reflect considerable solar radiation. Because clean glass produces film-type condensation, it is chosen instead of non-wettable plastics, which always produce drop-type condensation (21). The lower part of the frame is closed with transparent panes of glass or any suitable water-proof material. In the middle of the frame, a black porous evaporator frame is supported. Salt water is fed at the upper edge of the evaporator where it is distributed evenly. At the bottom end of the porous pad, the concentrated brine was collected in a "drip catch" channel and discharged through an outlet pipe. The inner

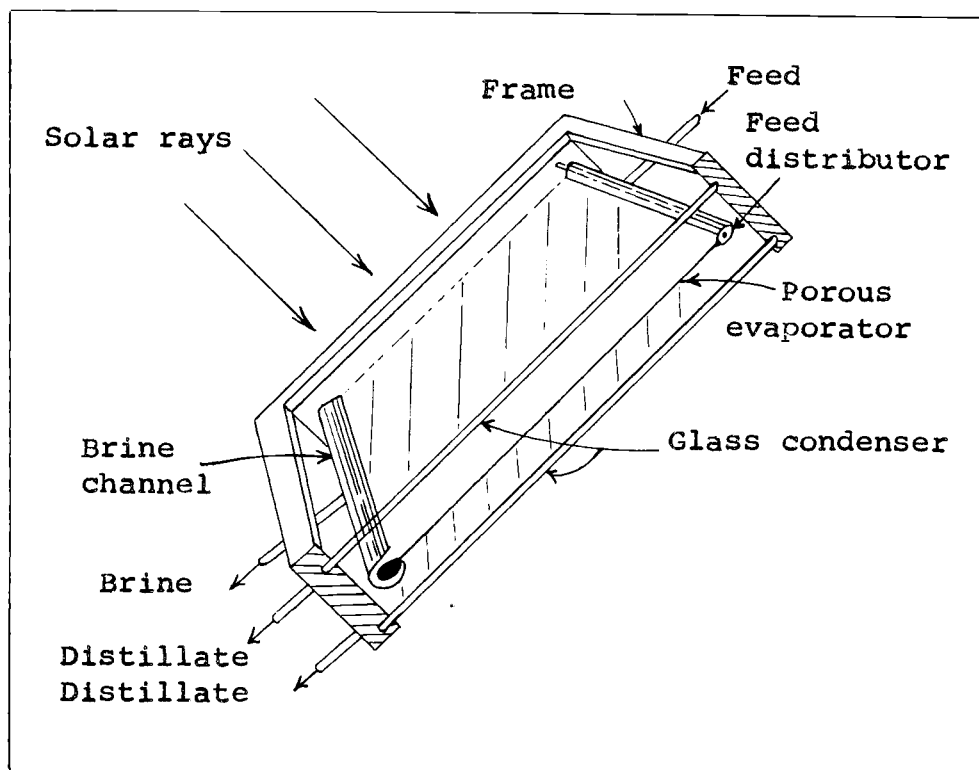


Figure 3: Schematic Cross Section of a
Flat Tilted Solar Still.

surface of the glass top and the inner back of the still served respectively as the front and back condensers.

A comparison between the respective efficiencies of the roof-type and tilted solar stills showed that the yield of the tilted solar still was 26 to 48 per cent greater than that of the horizontal still (2, 35).

4. Multiple-effect solar still. In the simple, roof-type still, the heat of condensation of the vapor on the glass cover is wasted, being carried away by the air and by radiation to the atmosphere. In a multiple effect still, solar radiation is reused to distill additional amounts of sea water. The incident radiation strikes a black absorber impervious to water vapor, below which there is a fabric acting as a wick, wetted slowly and continuously with sea water (see Figure 4). The vapors cannot rise through the impervious black absorber but move downward across a narrow air space and condense on a porous layer collecting the distillate, which is continuously withdrawn. A thin water-proof film made of coated sheet aluminum or Mylar serves as a transmitting medium for the heat of condensation. This heat of condensation serves to distill an additional amount of sea water from a second wick

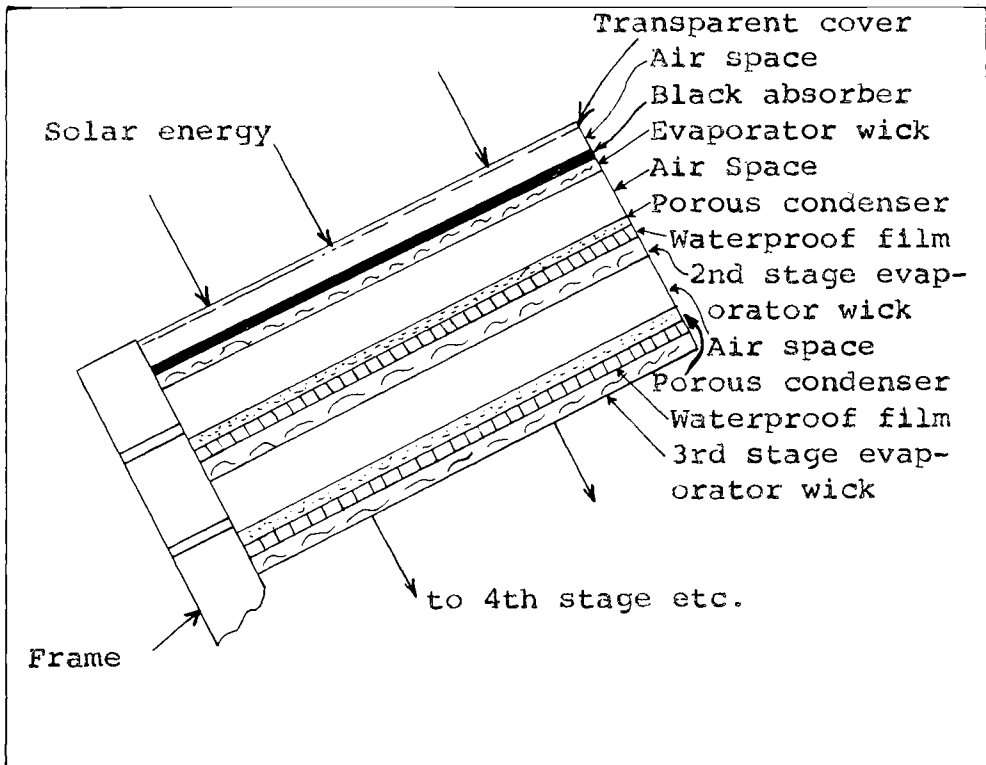


Figure 4: Diagram of a Multiple -
Effect Solar Still.

placed on the other side of the aluminum film. Several stages can be fixed in this manner and a temperature gradient is established in each stage. The temperature of the wicks is lower in each subsequent stage than in the one before. A three-effect multiple still produced 1.9 times more water than a single-effect tilted still of the same area (21).

5. Multiple-effect humidification process. This process differs from conventional distillation processes in that water vapor was first carried by dry air and then released by condensing on a cool surface. The source of energy may be solar or waste steam. The air used may be recirculated or fresh air could be introduced. Energy and mass transfer occur at temperatures below the normal boiling point of water.

Two major research programs are being conducted in this field: the first by Dr. Werner Grune at Georgia Institute of Technology, and the second by Hodges and Kassander at the University of Arizona (see Figure 5). Dr. Grune's research has been concerned mainly with a multiple-effect system which utilizes a collector-evaporator unit similar to the traditional solar still with air being

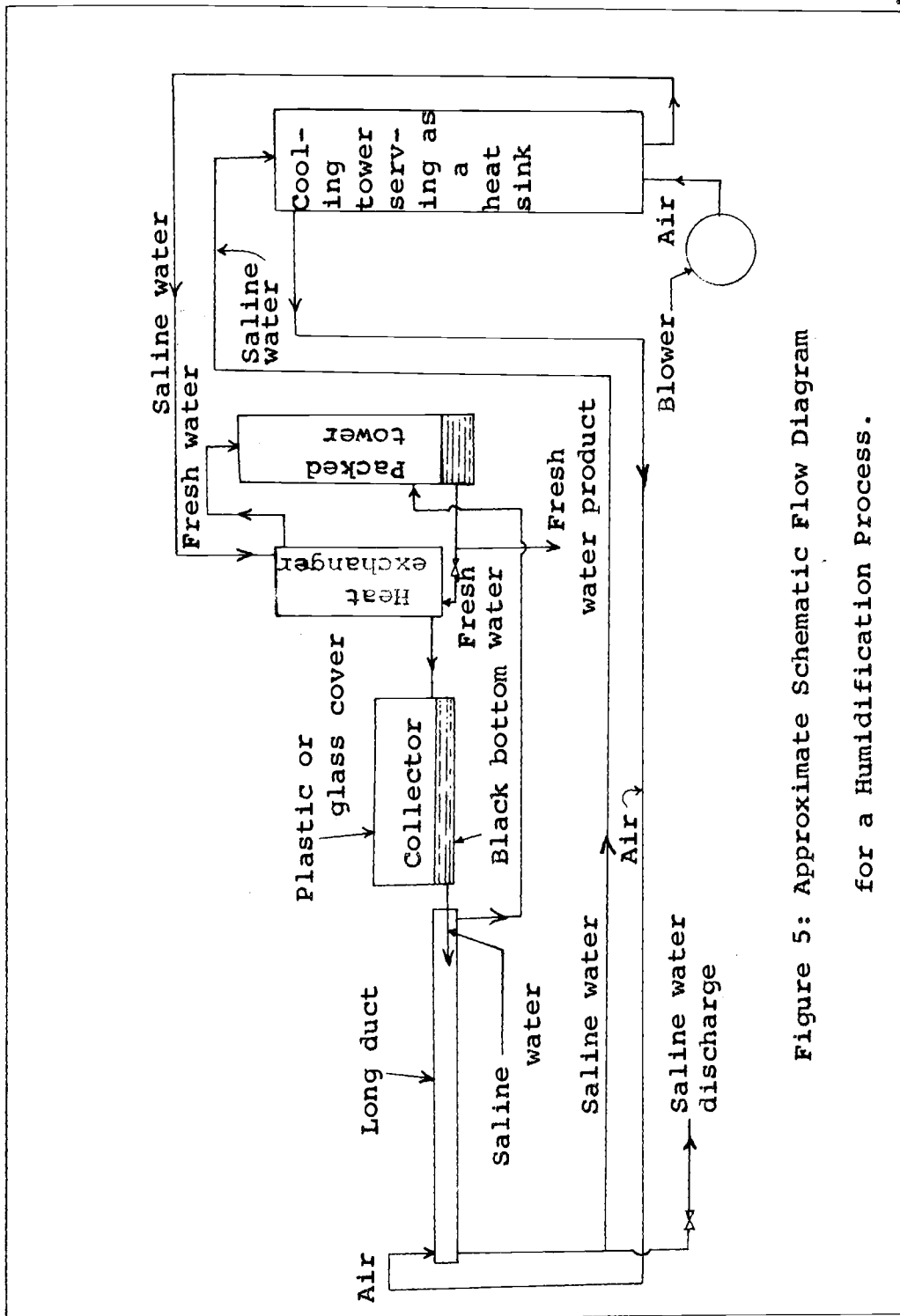


Figure 5: Approximate Schematic Flow Diagram for a Humidification Process.

blown over the still to create forced convection. An external condenser was used to permit the operation of the multiple-effect unit.

At the University of Arizona, the research conducted has stressed the separation of the collector, the evaporator, and the condenser. In principle, solar energy is received in the collector where heat is given to the salt water feed. The sea water from the collector is fed to a long duct, where relatively dry air is blown over the sea water. The air picks up moisture and the air and moisture are received by a condenser. The air gives up its moisture by condensation. The intake sea water coming from a cooling tower exchanges heat with the fresh water from the condenser where the condensate is cooled and the sea water is preheated. The air and sea water flow in a counter-current fashion (13, 31).

6. Portable solar still. A portable solar still has been described by the Russian scientist, Zaitsev (37), and it has the following features: The top of the still is a blackened metal surface (see Figure 6). A layer of fabric is attached along the inside of the metal surface. The still is tilted, and the sea water is fed to the fabric

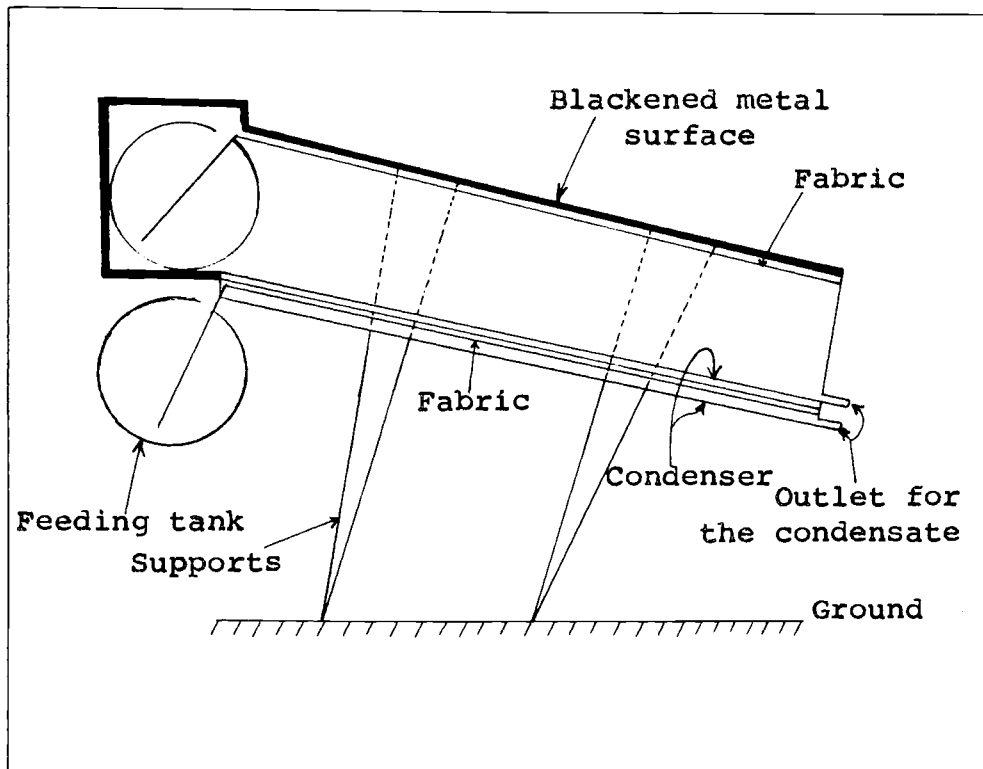


Figure 6: Schematic Diagram of a Portable Solar Still.

from a small tank located at the top of the inside of the still. An outside fabric layer is located along the bottom of the still, and this layer is fed from a small tank located at the outside of the still. Solar energy is received by the black surface, and the fabric is heated. The water vapor condenses along the bottom incline of the still, where it is directed to an outlet (37).

7. Vacuum desalinators of solar heater type.

Solar vacuum desalination is not discussed to any detail in the literature. The Russian scientist, Zaitsev, proposed a solar vacuum desalinator (37), where saline water is preheated to 60°C in a hot-house type solar water heater (see Figure 7). Hot water is fed to a moderately exhausted vacuum chamber where evaporation occurs. The vapor is condensed in a surface condenser. Fresh water is pumped to a storage tank, and the brine from the evaporator is directed to the sewer.

It is of interest to note that the above-mentioned processes have two common characteristics: low water yield and low efficiency. This research is conducted to improve the solar still efficiency and to increase the fresh water yield. The interest in this research is generated due to

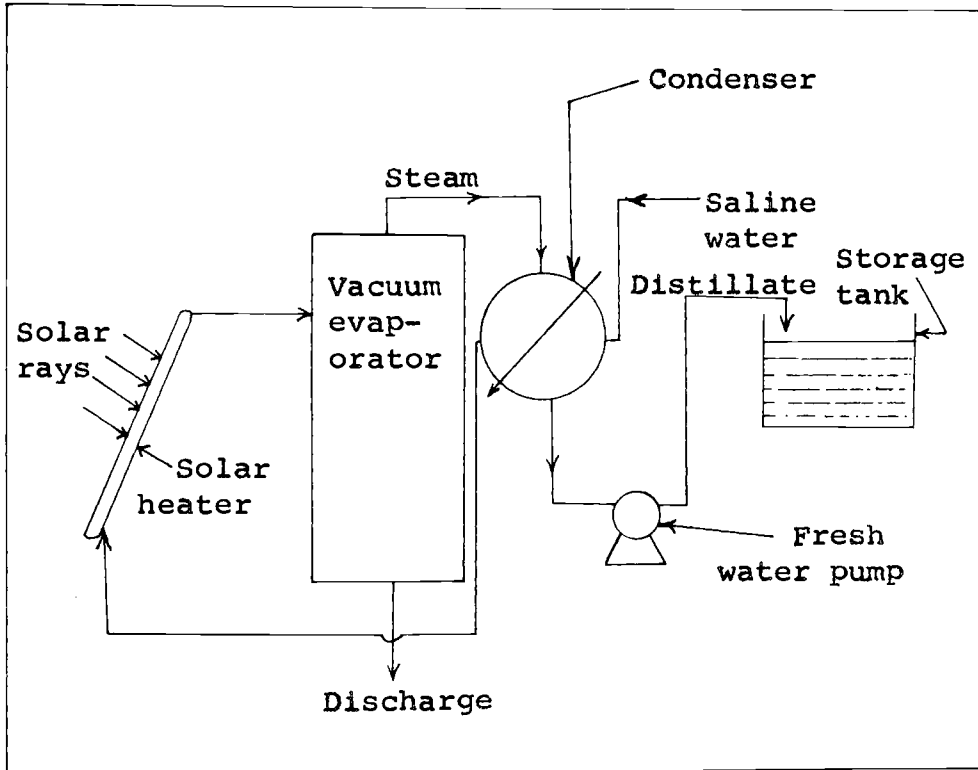


Figure 7: Flow Diagram for a Vacuum Desalinator
of Solar Heater Type.

the scarcity of literature related to solar vacuum desalination.

IV. PROPOSED SOLAR EVAPORATION PROCESS FOR SALINE WATER IN ARID REGIONS

A. Description of process

The proposed process of saline water conversion using solar energy and vacuum techniques is a new process in desalination research. Extended investigations of this process may render valuable contributions to the desalination problem as a whole. To be able to show the advantages of such a process, a generalized description is needed.

The theoretical development is concerned with a solar still of the "green-house" type in a desert location. The description of the "green-house" type solar still was presented in the Survey of Literature section. In all probability the solar still for the proposed process will lie flat on the ground or sand in order to have support for withstanding the necessary vacuum.(see Figure 8). Solar energy is transmitted through the transparent glass. This solar energy is absorbed by the black bottom of the still and directly released to the salt water in the basin. The water vapors formed are drawn to a separate condenser. The inerts in the system will be removed by a steam-jet or similar system.

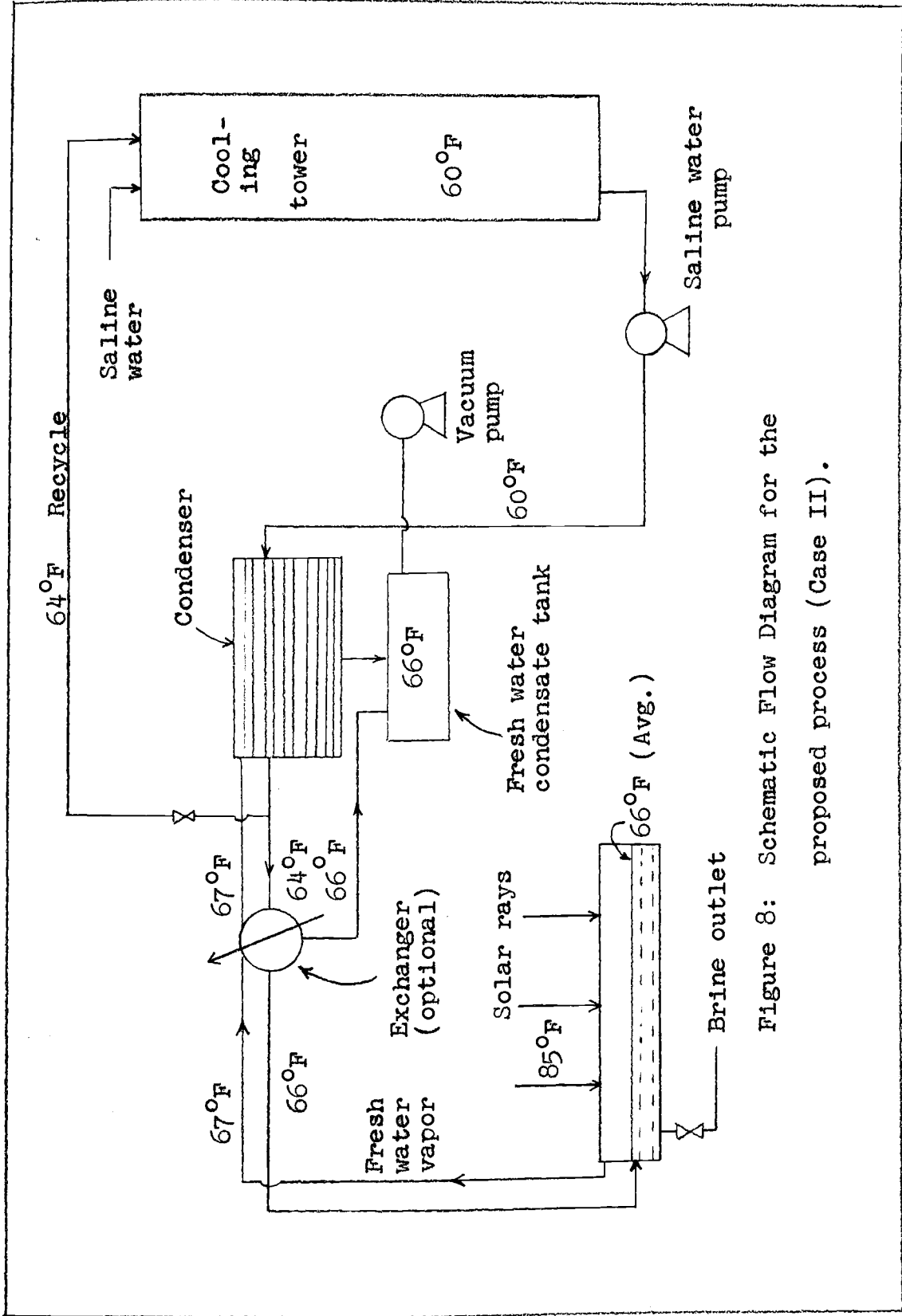


Figure 8: Schematic Flow Diagram for the proposed process (Case II).

The desired pressure (the vacuum) will correspond to the condensing temperature as supplied by the cooling tower water. Saline water and air may be in contact counter-currently in a standard cooling tower. There is a possibility that the water vapors can be condensed in coils placed in the bottom of the cooling tower, assuming that the physical location is not so distant as to give excessive pressure drop.

B. General calculations and assumptions

The mathematical development of the theory involved is simplified in this section. A detailed mathematical analysis for different cases is shown in the Discussion and the Appendix. The following simplifications and assumptions could be modified to meet special needs of a research program using solar energy and vacuum techniques for saline water conversion.

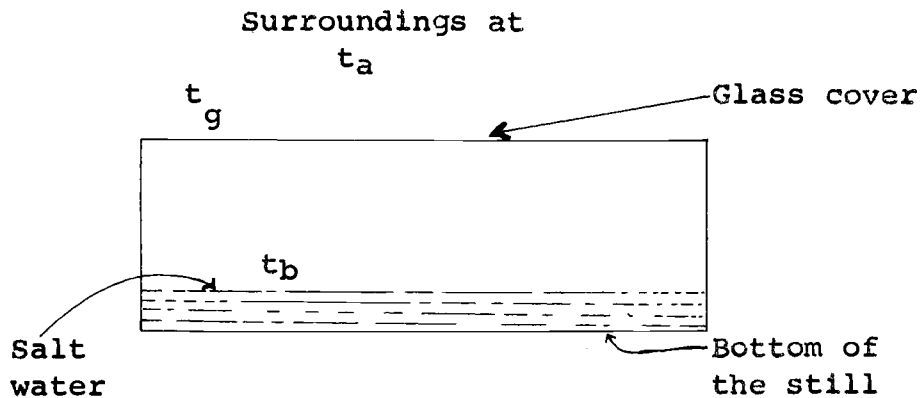
To account for the energy distribution in a solar still similar to the one described above, the average glass cover temperature should be first estimated. In general t_a and t_b could be assumed and t_g could be estimated.

Where,

t_a = Temperature of the air surrounding the still
(°F.).

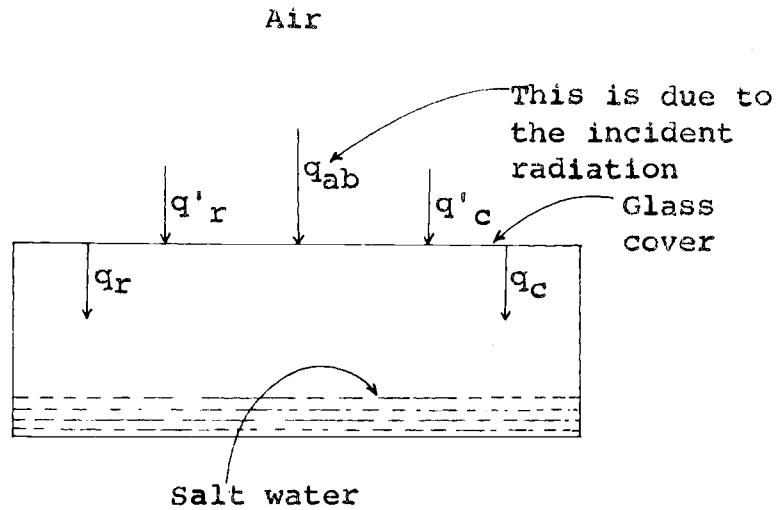
t_b = Equilibrium temperature of the water in the basin ($^{\circ}\text{F.}$).

t_g = Average glass cover temperature ($^{\circ}\text{F.}$).



In order to estimate t_g , a heat balance around the glass cover of the still may be considered. The glass cover receives heat by radiation and convection from the surrounding atmosphere and also by absorption of a fraction of the incident solar energy. The glass cover transmits heat by radiation and convection to the inside of the still. The heat balance around the glass cover may then be written as follows.

$$q'_r + q'_c + q_{ab} = q_r + q_c \quad (1)$$



Where,

q'_r = Net rate of radiation interchange from the air to the glass cover (Btu/ft²-hr).

q'_c = Net rate of heat transfer by convection from the air to the glass cover (Btu/ft²-hr).

q_{ab} = Rate of heat absorbed by the cover from the incident solar energy (Btu/ft²-hr).

q_r = Net rate of radiation interchange from the glass cover to the water basin (Btu/ft²-hr).

q_c = Net rate of natural convection heat transfer from glass cover to the vapor inside the still (Btu/ft²-hr).

It is now necessary to find the values of the different components of Equation (1). Heat transfer rates by radia-

tion may be calculated as follows:

$$-q'_r = \sigma \epsilon (T_g^4 - T_a^4) \quad (2)$$

Where,

σ = Stefan-Boltzmann constant = 0.1713×10^{-8}
(Btu/ft²-hr-(°R)⁴).

ϵ = Emissivity of glass.

T_g = Average absolute temperature of the glass cover
(°R).

T_a = Absolute temperature of the surrounding air (°R).

The net rate of heat transfer by convection may be calculated as follows:

$$q'_c = h'_c (t_g - t_a) \quad (3)$$

Where,

h'_c = Convection heat transfer coefficient from the
surrounding air to the glass cover (Btu/ft²-hr-
°F).

To find h'_c the following equation was taken from Symposium on Saline Water Conversion, 1957, reference 21 pages 140 and 142.

$$h'_c = 0.99 + 0.21V \text{ under practical conditions} \\ \text{subject to wind} \quad (4)$$

Where,

V = Wind velocity (ft/sec).

This is an empirical relation which is fitted by the data taken from Table Number two of the above mentioned reference. Since in this proposed process the temperature gradient between the air and the glass cover is small, the heat transferred from the air to the glass cover is relatively small. Thus, the error introduced by using Equation (4) is very small. The rate of heat absorbed by the cover from the incident solar energy was found by the following relation:

$$q_{ab} = (q_1) (\alpha) \quad (5)$$

Where,

q_1 = Incident radiation on the glass cover (Btu/ft²-hr).

α = Absorptivity of the glass cover.

The net radiation interchange between the glass cover and the water in the basin is:

$$q_r = (0.1713 \times 10^{-8}) (0.937) (T_g^4 - T_b^4) \quad (6)$$

Where,

0.937 = Glass emissivity from reference (1), page 162.

T_b = Absolute temperature of the water basin (^oR).

It is assumed that there is a slow rate of mass transfer inside the still. Thus, the rate of natural convection heat transfer from the glass cover to the water in the basin is approximated by the equation:

$$q_c = 0.256 (t_g - t_b)^{\frac{1}{4}} (t_g - t_b) \quad (7)$$

This equation is taken from reference (1) page 162. This energy is transferred to the water in the basin, and its magnitude may be slightly larger in the case of forced convection. Thus, the value given by equation (7) is on the safe side. If the dimensions of the apparatus are well defined, q_c may be calculated by using the appropriate heat transfer coefficient. In this case more heat from the glass cover may be added to the total amount of heat available for water evaporation, and this provides more contribution toward the advantages of the basic process. After replacing q'_r , q'_c , q_r , and q_c in Equation (1) by their corresponding values, the following equation may be obtained:

$$\begin{aligned} -0.162 \left[\left(\frac{T_g}{100} \right)^4 - \left(\frac{T_a}{100} \right)^4 \right] - h'_c (t_g - t_a) + q_{ab} = \\ 0.162 \left[\left(\frac{T_g}{100} \right)^4 - \left(\frac{T_b}{100} \right)^4 \right] + 0.256 (t_g - t_b)^{\frac{1}{4}} (t_g - t_b) \quad (8) \end{aligned}$$

Equation (8) may be solved by trial and error to find the average temperature of the glass cover.

The heat loss or gain by conduction from the water basin and the walls of the still to the surrounding atmosphere may be found by the general relation:

$$Q = k_m A_m \frac{\Delta t}{\Delta x} \quad (9)$$

Where,

Q = Heat loss or gain by conduction (Btu/hr).

k_m = Mean thermal conductivity of the insulation (Btu/ft-hr-°F).

A_m = Logarithmic mean cross-sectional area of insulation perpendicular to the direction of flow heat (ft²).

Δt = Temperature gradient (°F.).

Δx = Insulation thickness (ft).

Two different cases are considered. The following is assumed for the first case:

The basin water temperature is $t_b = 84^\circ\text{F}$,

The air temperature is $t_a = 85^\circ\text{F}$.

In the second case, the following assumptions were made:

$t_b = 65^\circ\text{F}$,

$$t_a = 85^{\circ}\text{F.}$$

The mathematical equations in the previous pages were used to estimate the average temperature of the glass cover. To determine the energy distribution within the solar still the following assumptions are made:

1. The cover of the still is made of plate glass.
2. The area of the cover of the still is equal to the area of the bottom of the water basin.
3. The basin is large and the operation is performed at steady-state.
4. The heat loss or gain by conduction from the walls of the still to the surrounding atmosphere is neglected.
5. The temperature of the cover is an average temperature based on neglecting the temperature drop through the thickness of the glass.
6. The absorptivity of the glass cover is 0.11.
7. The transmission of the glass cover is assumed to be 77 per cent.
8. The average solar radiation is 1800 (Btu/ft²-12 hr. day).

9. The wind velocity is one mile per hour, and $h'_c = 1.30$ (Btu/ft²-hr-°F).
10. The basis for calculation is one square foot of basin area.

C. Calculated cases

Case 1. For this case $t_b = 84^\circ\text{F}$ and $t_a = 85^\circ\text{F}$. Solve for t_g by using Equation (8).

$$T_b = 84 + 460 = 544^\circ\text{R}$$

$$T_a = 85 + 460 = 545^\circ\text{R}$$

First assumption: Assume $t_g = 88^\circ\text{F}$

$$T_g = 88 + 460 = 548^\circ\text{R}$$

$$146.1 - 142.9 + 3.9 + 146.1 - 141.8 + 1.45 \stackrel{?}{=} 16.5$$

$$297.55 - 284.7 \stackrel{?}{=} 16.5$$

$$12.85 \stackrel{?}{=} 16.5$$

The number to the right represents the heat absorbed by the glass cover and it is equal to the product of the incident radiation and the absorptivity of the glass.

Second assumption: Assume $t_g = 90^\circ\text{F}$

$$T_g = 90 + 460 = 550^\circ\text{R}$$

$$148.2 - 142.9 + 6.5 = 148.2 - 141.8 + 2.4 \stackrel{?}{=} 16.5$$

$$305.3 - 284.7 \stackrel{?}{=} 16.5$$

$$20.6 \stackrel{?}{=} 16.5$$

Third Assumption: Assume $t_g = 89^\circ\text{F}$

$$T_g = 549^\circ\text{R}$$

$$147.2 - 142.9 + 5.2 = 147.2 - 141.8 + 1.9 \stackrel{?}{=} 16.5$$

$$305.5 - 284.7 \stackrel{?}{=} 16.5$$

$$16.8 \stackrel{?}{=} 16.5$$

Thus, for the first case $t_g = 89^\circ\text{F}$. The results of these trials are shown in Table II on the following page.

The solution for the rate of heat transfer by radiation from the cover to the basin is then:

$$q = \sigma \epsilon (T_g^4 - T_b^4)$$

$$\sigma = 0.1713 \times 10^{-8}$$

$$\epsilon = 0.937$$

$$q_r = 0.162 \left[(5.49)^4 - (5.43)^4 \right]$$

$$q_r = 0.162 (908 - 866) = 0.162 (42)$$

$$q_r = 6.8 \text{ (Btu/ft}^2\text{-hr)}.$$

The heat transfer by convection from the glass cover is:

$$q_c = 0.256 (t_g - t_b)^{\frac{1}{4}} (t_g - t_b)$$

$$q_c = 0.256 (89 - 84)^{\frac{1}{4}} (89 - 84)$$

$$q_c = 0.256 (5)^{\frac{1}{4}} (5) = 1.9 \text{ (Btu/ft}^2\text{-hr)}.$$

Since the incident radiation is assumed to be 1800

TABLE II
ESTIMATION OF THE AVERAGE
GLASS COVER TEMPERATURE FOR THE
PROPOSED PROCESS

$$t_a = 85^{\circ}\text{F}$$

$$t_b = 84^{\circ}\text{F}$$

Trial Number	t_g (°F.)	q'_r *	q'_c	q_{ab}	q_r	q_c
1	88	3.20	3.90	16.5	4.30	1.45
2	90	5.30	6.50	16.5	6.40	2.40
3	89	4.30	5.20	16.5	5.40	1.90

* All q 's have the units of (Btu/ft²-hr).

(Btu/ft²-12 hrs), the energy transmitted is:

$$1800 \times \frac{77}{100} = 1389 \text{ (Btu/12 hrs)}$$

Energy reflected from the still:

$$1800 \times \frac{12}{100} = 215 \text{ (Btu/12 hrs)}$$

Energy absorbed by the glass cover:

$$1800 \times 0.11 = 198 \text{ (Btu/12 hrs)}$$

The total amount of energy available for evaporation is:

$$\begin{aligned} q_{\text{avail}} &= (1389) + (1.9)(12) + (6.8)(12) = 1389 + 22.8 + 81.6 \\ &= 1493.4 \text{ (Btu/12 hrs)} \end{aligned}$$

or,

$$\frac{1493.4}{1800} \times 100 = 83.0\%$$

The energy distribution for the incident radiation is as follows:

<u>Distribution</u>	<u>% of Solar Radiation</u>
Evaporation	83.0
Solar radiation reflected by still	12.0
Radiation and convection losses from the glass cover to the atmosphere	$\frac{5.0}{100.0}$

For the deep basin solar still described in reference (1) pages 166-172, the heat available for water evaporation was 32%.

A process using the basic principle of this research will have 2.6 times more heat available for water evaporation than the most promising distillation unit in existence.

Case 2.

$$T_b = 65 + 460 = 525^{\circ}\text{R}$$

$$T_a = 85 + 460 = 545^{\circ}\text{R}$$

Solve for t_g by trial and error from Equation (8).

$$\text{Assume } t_g = 81^{\circ}\text{F}$$

or,

$$T_g = 81 + 460 = 541^{\circ}\text{R}$$

Replace, t_a , t_b , and t_g by their values in Equation (8) and check to see if both sides of the equation are equal:

$$\begin{aligned} T_g = 81 + 460 = 541^{\circ}\text{R}, \quad t_b = 525^{\circ}\text{R}, \quad t_a = 545^{\circ}\text{R} \\ -0.162 \left[(5.41)^4 - (5.45)^4 \right] - 1.30(81 - 85) + 16.5 \\ \stackrel{?}{=} 0.162 \left[(5.41)^4 - (5.45)^4 \right] + 0.256(81 - 65)^{\frac{1}{4}}(81-65) \end{aligned}$$

or,

$$\begin{aligned} -138.8 + 142.9 + 5.2 + 16.5 \stackrel{?}{=} 138.8 - 123.0 + 8.2 \\ 25.8 \stackrel{?}{=} 24.0 \end{aligned}$$

This result was reached after applying a series of trials.

Thus, for this case t_g is 81°F .

$$q_r = 0.162 \left[(5.41)^4 - (5.25)^4 \right]$$

$$q_r = 0.162 (860 - 760)$$

$$q_r = 16.2 \text{ (Btu/ft}^2\text{-hr)}$$

and,

$$q_c = (0.256) (81 - 65)^{\frac{1}{4}} (81 - 65)$$

$$q_c = (0.256) (16)^{\frac{1}{4}} (16) = 8.2 \text{ (Btu/ft}^2\text{-hr)}$$

$$q_r + q_c = 16.2 + 8.2 = 24.4 \text{ (Btu/ft}^2\text{-hr)}$$

For a 12 hour period:

$$q_r + q_c = 24.4 \times 12 = 293 \text{ (Btu/12 hrs)}$$

The total amount of energy available for water evaporation is:

$$1389 + 293 = 1682 \text{ (Btu/12 hrs)}$$

or,

$$\frac{1682}{1800} \times 100 = 93.5\% \text{ of the incident radiation.}$$

This amount of heat available for water evaporation is higher than the previous case, due to convection and radiation gains from the surroundings. Although conduction gains are neglected, under these conditions a process applying the basic principle of this research will produce 2.92 times more fresh water than the best promising solar distillation unit.

The scarcity of literature in the field of saline water conversion using solar energy and vacuum techniques, makes the proposed process in this section very attractive

for further research. This proposed process produces on the average 2.76 times more fresh water than the most promising solar distillation unit.

V. DESCRIPTION OF APPARATUS

The apparatus used for the investigation of saline water conversion by the application of vacuum and solar energy is described in detail in this section. The evaporation vessel was covered with a transparent Plexiglas surface. A graduated column was attached to the main vessel (see Figures 9 and 10). When water was fed into the main vessel, the application of light by using an infrared lamp and the application of vacuum by using a vacuum pump caused evaporation. Water vapor leaving the evaporator entered a condenser where it was condensed and collected in a receiving chamber. An air blower served to blow air across the top of the Plexiglas cover at an average speed of one and a half miles per hour. An air meter was used to measure the air velocity, and the average radiation on the top Plexiglas surface was obtained by using an Eppley radiation pyrhelio-meter. Thermocouples were used to determine the temperatures of interest in the system, and a pump was used to discharge

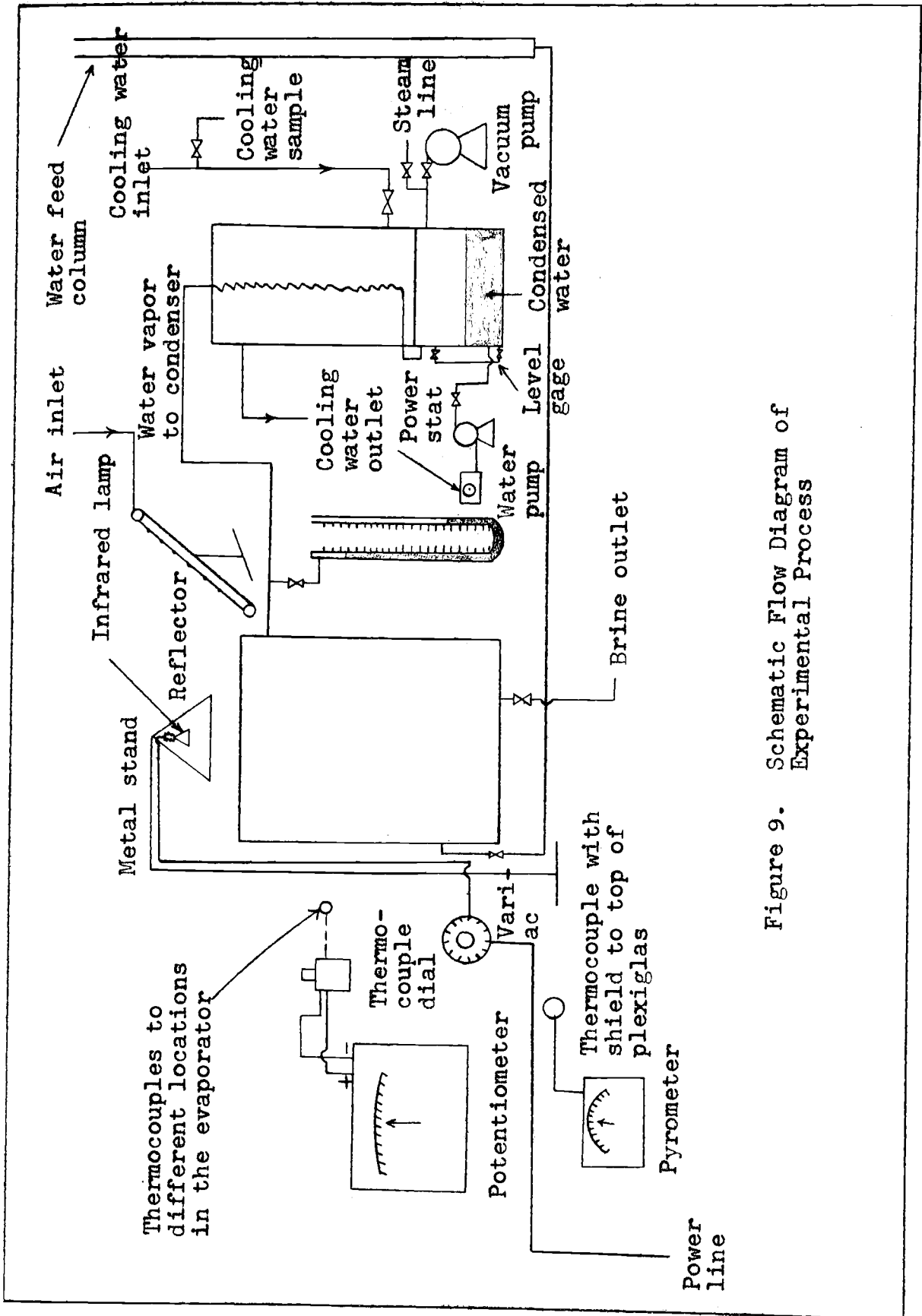


Figure 9. Schematic Flow Diagram of Experimental Process

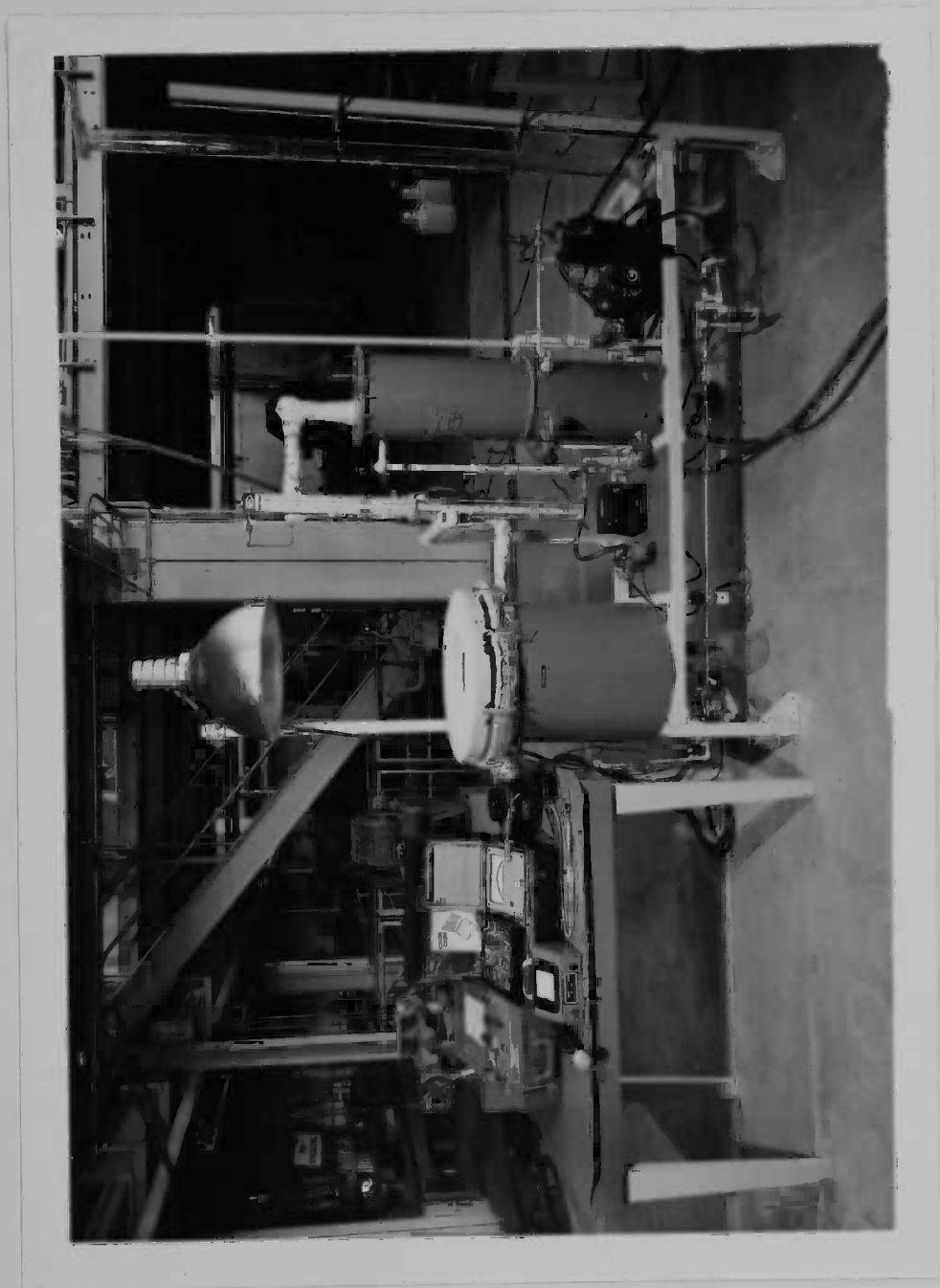


Figure 10. Photograph of Apparatus

the fresh water collected.

A detailed description of the respective sections of the apparatus is presented in the following pages.

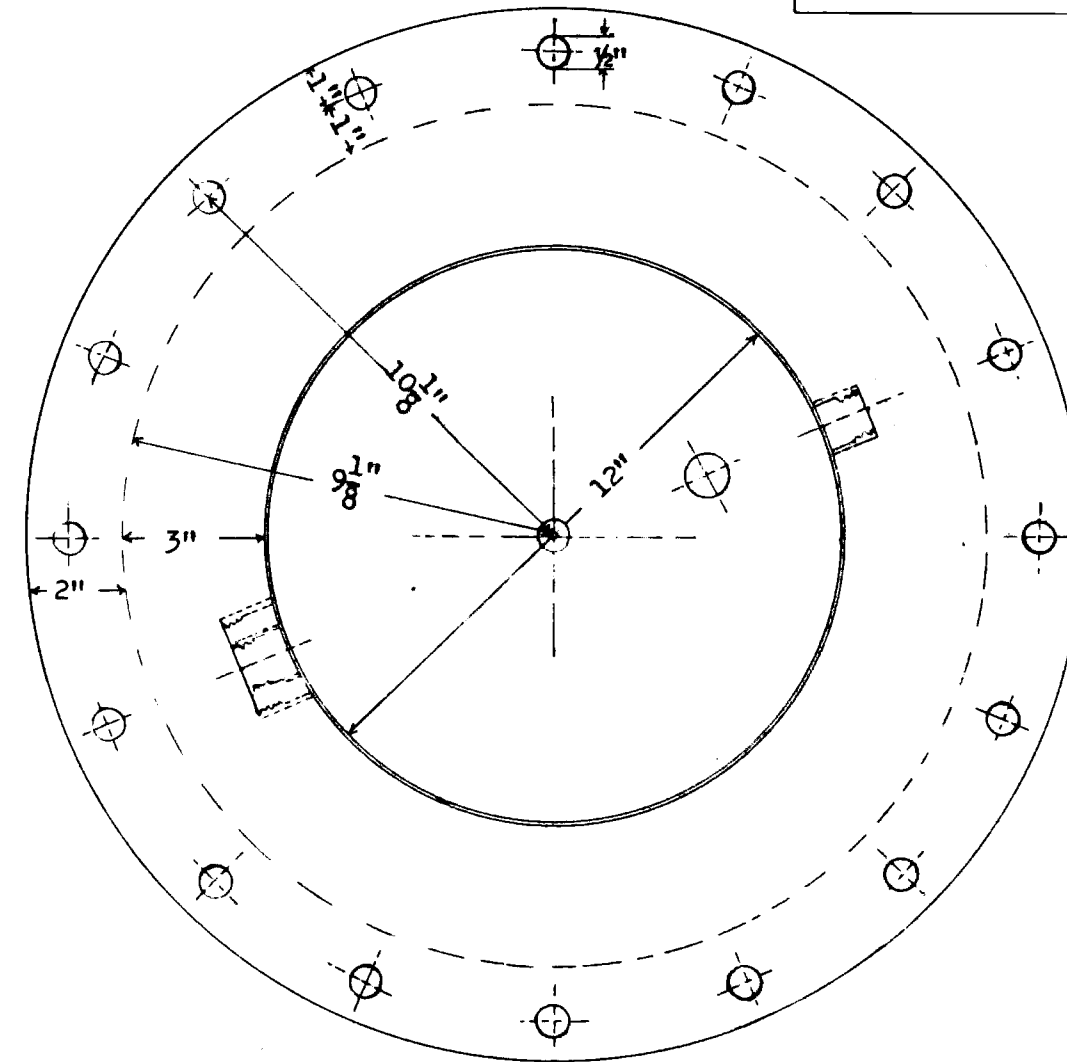
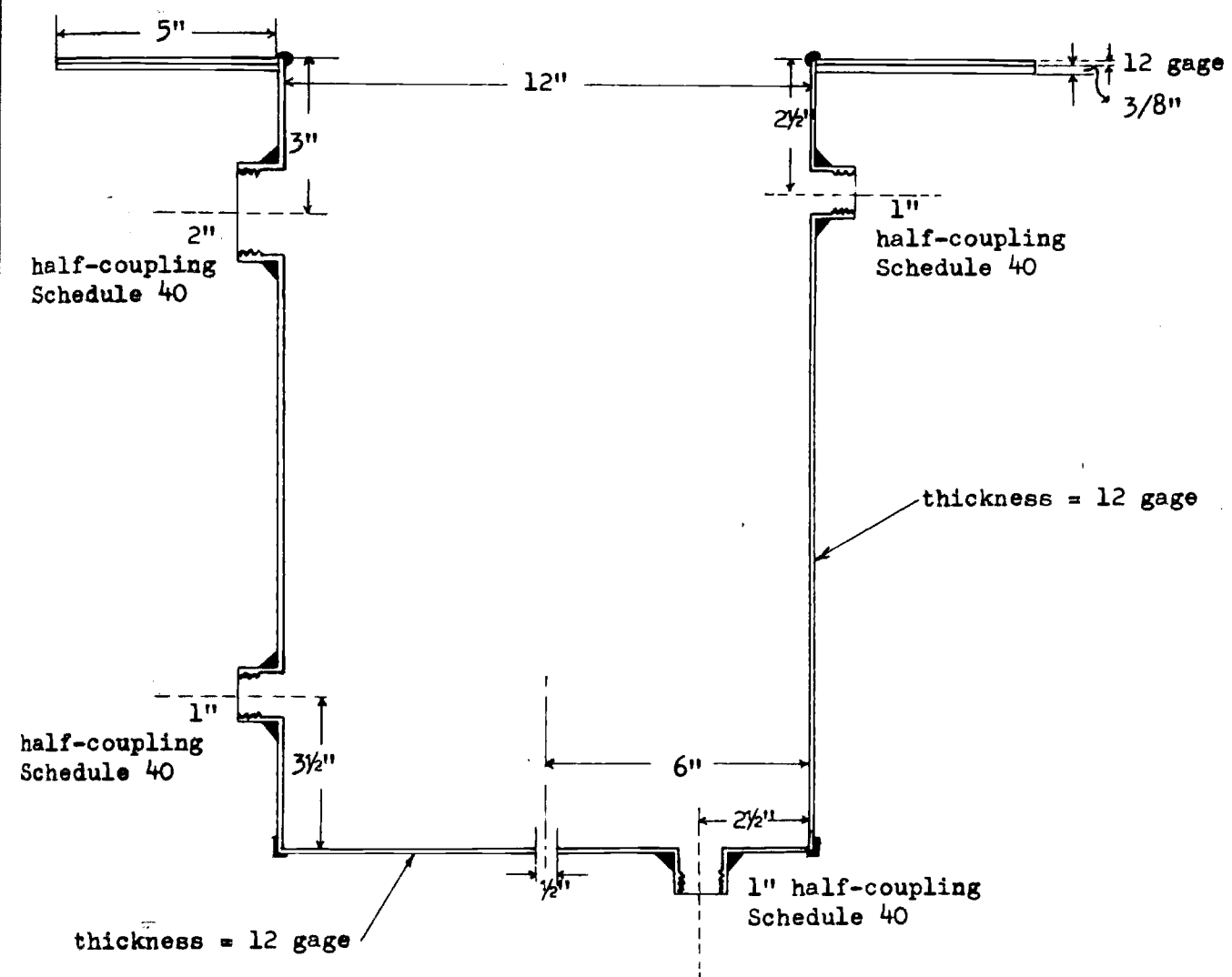
A. Evaporator

The vessel constituted an evaporator with no heat transfer surface inside. Energy in the form of infrared radiation was transmitted through the Plexiglas cover.

The evaporation of water was carried out in a vessel made of K-Monel, 1/10-inch thick (see Figure 11). Extending around the top of the vessel was a metal flange. The upper part of this flange was K-Monel 1/10-inch thick, and it was welded to the vessel along the inner side. The lower part of the flange was a ring support which was welded to the Monel flange in eight points equally spaced. On top of this flange, a rubber gasket was placed. A circular piece of Plexiglas II UVA (ultraviolet absorbing) was laid on top of the rubber gasket. The Plexiglas served as a cover on the top of the evaporator. The Plexiglas disk was $\frac{1}{2}$ -inch thick and 17-inches in diameter. The Plexiglas was fastened to the flange by eight "C"-clamps equally spaced. This arrangement with the aid of nonhardening Permatex between the cover and the gasket and between the

FRONT VIEW

TOP VIEW



THE UNIVERSITY OF ARIZONA
Dept. of Chemical Engineering

Title: Main Inner Cylinder
(Evaporator)

Drawn By: Esber I. Shaheen

Scale: Four inches are equivalent
to one inch on the graph

Date: July 24, 1963

Figure 1: Sketch of The Inner Cylinder (Evaporator)

gasket and the flange prevented air leakage. Microlite or glass wool insulation, 3-inches thick, was wrapped around the cylinder. This insulation fitted between the inner cylinder and an outer cylinder. The density of this insulation was 0.75 lb/ft^3 , and its thermal conductivity as a function of temperature was found in reference (16). The outer cylinder was made of 22 gauge galvanized steel and served to contain the insulation and thermocouple assembly (see Figure 12).

B. Condenser

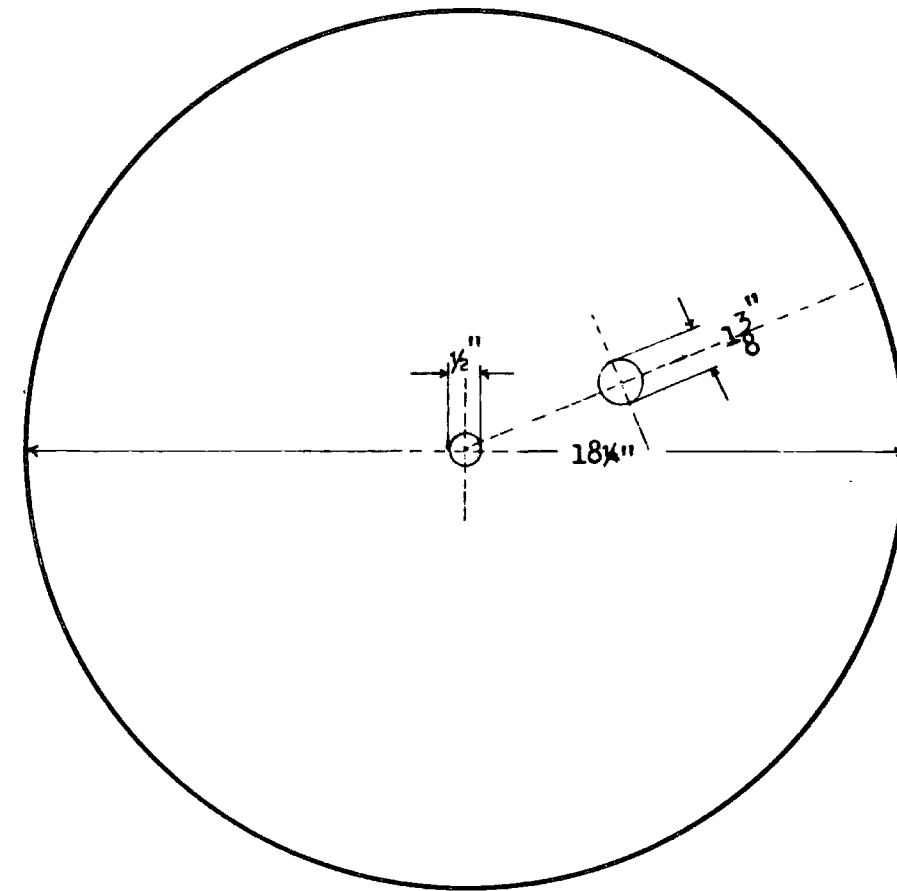
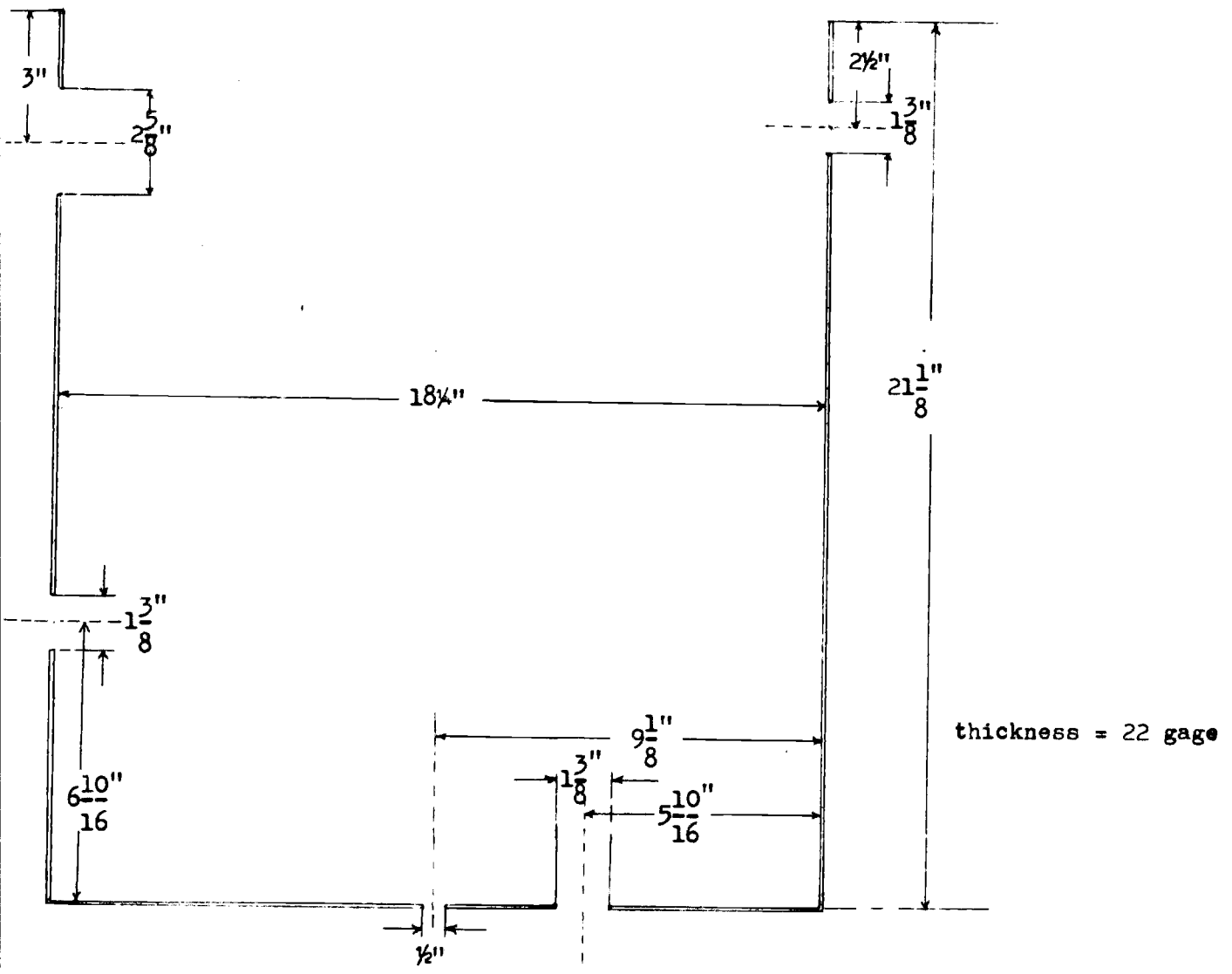
The condenser used was manufactured by Buflovak Equipment Division of Blaw-Knox Company. This was a copper coil condenser consisting of a copper coil, $\frac{1}{4}$ -inch in diameter, mounted in a sheet steel tank with the lower part forming the receiver. There were approximately five square feet of surface in the coil, and the receiver held approximately four gallons. The condenser was 3-feet long and 10-inches in diameter.

C. Pumps

The vacuum in the system was established using Number 927 vacuum pump, manufactured by Nelson Vacuum Pump Company. Cooling water was used when the unit was operated

FRONT VIEW

TOP VIEW



thickness = 22 gage

THE UNIVERSITY OF ARIZONA
Dept. of Chemical Engineering

Title: Outer Cylinder
(Insulation cover)

Drawn By: Esber I. Shaheen

Scale: Four inches are equivalent
to one inch on the graph

Date: July 24, 1963

Figure 12: Sketch of The Outer Cylinder Section

with high surrounding temperatures.

The fresh water collected in the collection chamber of the condenser was taken out by using a pump with 1/8-inch fittings made by Cole Parmer Instrument and Equipment Company. This pump was a 7025 Roll-Flex pump with an electronic speed controller. The powerstat, which had a scale of 0-100 divisions permitted the control of flow rate from 90 to 500 milliliters per minute.

D. Feed Column

Plexiglas tubing 2-inches in diameter and five and a half feet long was used as a feed column. It was calibrated by attaching along the length of the cylinder a length of graph paper. The equivalent of each division on the graph paper was determined in milliliters of fresh water.

E. Air Blower

A piece of 2-inch pipe was connected to the 40 pounds per square inch air supply in the laboratory. Starting at four inches from the end of the pipe nine small holes were drilled. This arrangement was used to blow the air along the top of the cylinder, thus simulating wind which might be encountered in the case of an outdoor still.

F. Electric System

A General Electric Infrared Lamp 1M/T40/3, 1000-watts, was used, with a voltage range of 115-125 volts. The light center length of the lamp was 3 and 1/16-inches, and the overall length was 7 and 1/4-inches.

A 17½-inch number 3050A Steber reflector was used (see Figure 13). Different lamps could be fitted into an exchangeable socket located at the top of the reflector. The reflector was fitted to a post in such a way that the distance between the reflector and the top of the evaporator could be varied as desired. The voltage of the infrared lamp used was controlled by a Variac which had a voltage scale with a range of zero to 130 volts, and the voltage scale was divided into ten-volt increments with each division being equivalent to two volts.

G. Thermocouples

Temperatures at several points in the evaporator were measured by using copper-constantan thermocouples. The wires of the thermocouples, number 24-55-1, were manufactured by Leeds and Northrup Company and were attached to a selector switch. Each number on the selector switch corresponded to a specific thermocouple in the system.



Figure 13. Photograph of the Infrared Lamp
and its Reflector

The locations of the various thermocouples are shown in Figure 14. A Leeds and Northrup potentiometer was used for determining the potential difference developed by the respective thermocouples.

H. Air-Meter

The wind velocity across the Plexiglas cover was measured by an air draft indicator, Model R-2, manufactured by Hastings-Raydist, Inc.

The Hastings Model R-2 air draft indicator consisted of two basic units, the indicating unit and the velocity pickup, generally referred to as the probe.

The air-meter consisted of a noble metal thermopile placed in the air stream. The hot junctions of the thermopile were heated by an alternating current, while the cold junctions were insulated by heavy mounting studs of low thermal conductivity. A d-c voltage was thereby generated between the hot and cold junctions.

Thermal difference was a measure of the velocity of the air stream into which the thermopile was inserted. Flow of air past the thermopile tended to reduce the temperature of the hot junctions and thereby reduced the d-c volt-

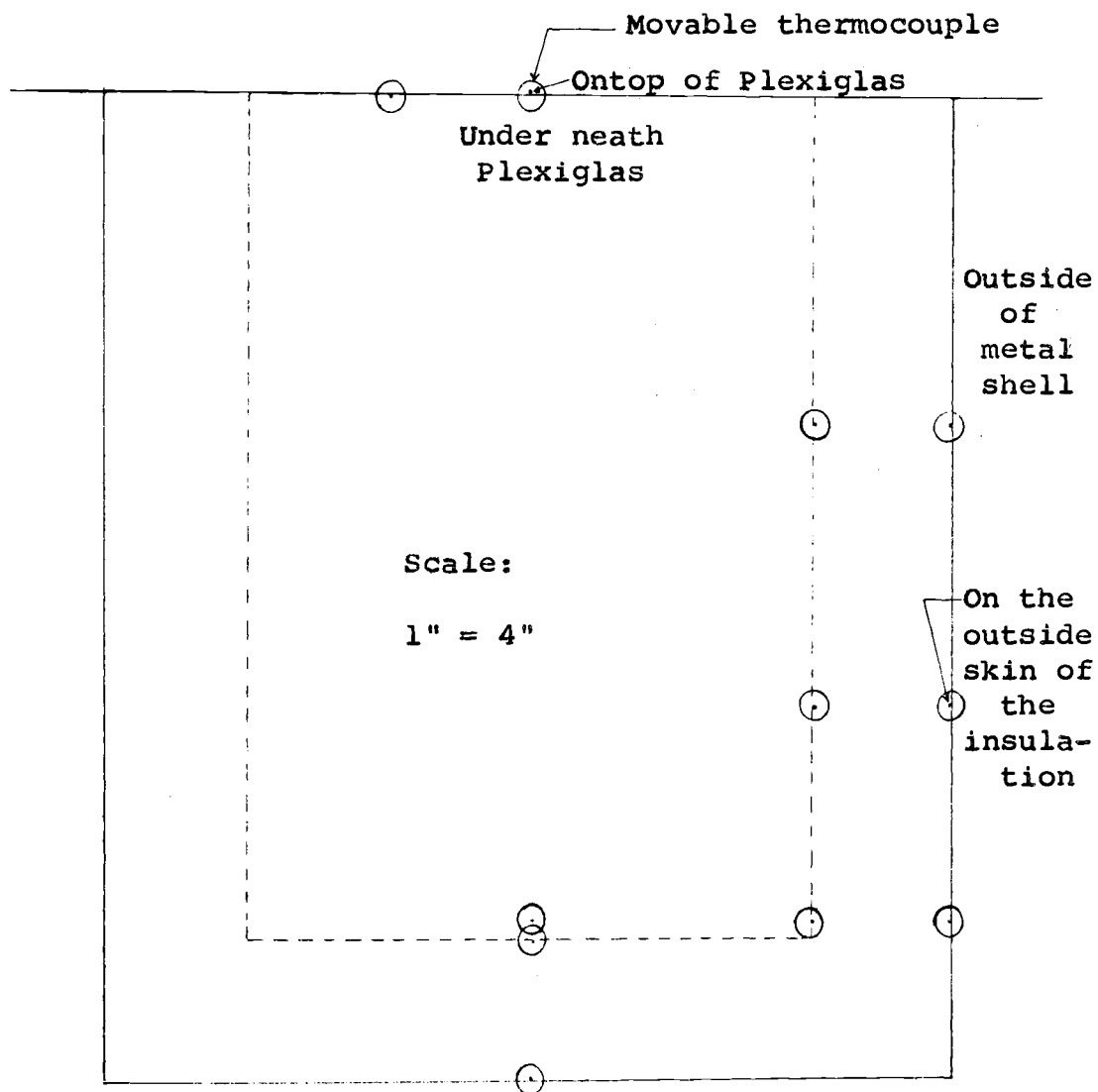


Figure 14: Distribution of Thermocouples Around the Evaporator.

age output. This output voltage was calibrated to indicate air velocity.

I. Epply radiation pyrhelometer

The sensitive elements in this radiation pyrhelometer were copper-constantan thermocouples, faced with a blackened non-selectively absorbing disk. The electromagnetic force (averaging approximately two millivolts generated per gram calorie of radiation) in all cases was measured by a recording potentiometer. This pyrhelometer is owned by the Solar Laboratory of the University of Arizona, and it was made by Eppley laboratory, Newport, Rhode Island.

J. Flow system

All piping in the system was made of galvanized steel. Cooling water to the condenser entered through a $\frac{1}{2}$ -inch pipe (see Figure 9). A $\frac{1}{4}$ -inch hoke valve was installed between the condenser and the vacuum pump, and it was used to control the pressure inside the system. In order to prevent vapor-lock, steam was used for start-up operation.

Water vapor from the evaporator flowed through a $\frac{1}{2}$ -inch pipe. A 36-inch U-tube manometer was installed in this line for the purpose of measuring pressure. A $\frac{1}{4}$ -inch

valve was installed between the collecting chamber of the condenser and the withdrawal pump.

Rubber tubing was used to connect the cooling water line to the water fittings on the vacuum pump and to connect the withdrawal pump to the condenser collecting chamber.

The air flow to the "blower" was controlled by a $\frac{1}{2}$ -inch hoke valve.

VI. PROCEDURE

A. Calibrations

Copper-constantan thermocouples were used for temperature measurements in the system. The thermocouples were calibrated by using the following procedure. About 500 milliliters of water were placed in a 1000-milliliter beaker. The temperature of the water bath was increased at different time intervals. A thermometer was placed in the beaker, and the thermocouples were placed near the mercury reservoir of the thermometer. Corresponding to each increase in temperature, the thermometer reading and the potentiometer reading for each thermocouple were recorded. The thermometer used in the calibration procedure was checked against a standardized thermometer. A graph of the correct thermometer temperature readings versus potentiometer readings in millivolts was prepared separately for each of the ten thermocouples, (see Figure 15 for an example).

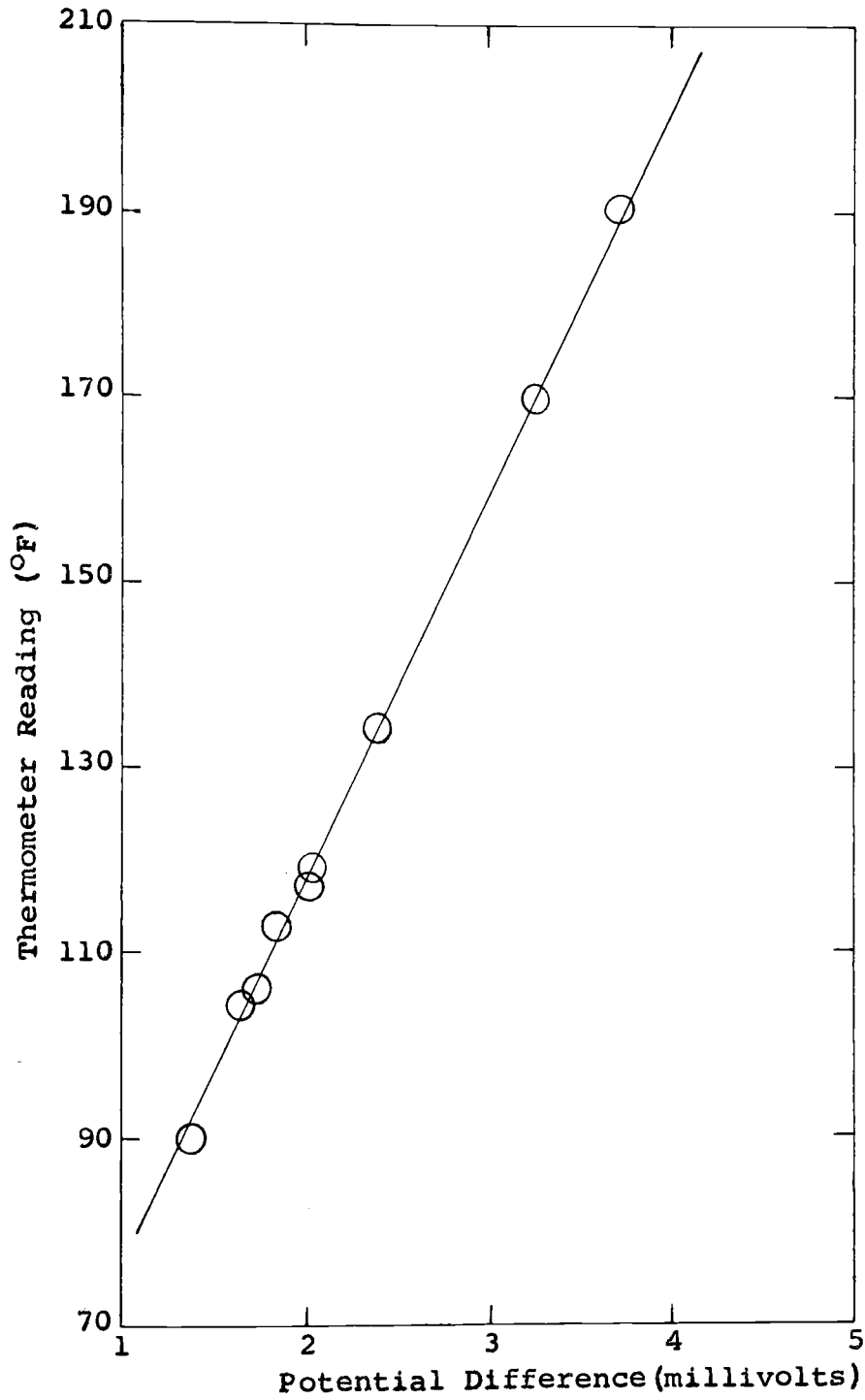


Figure 15: Thermocouple Calibration.

Thermocouple Number 0.

The feed column was calibrated by attaching against its length a graph paper with ten divisions in each square. An amount of 3000 milliliter of distilled water was fed to the column and the total number of divisions corresponding to the height of water was found. Each division corresponded to approximately 5.16 milliliters.

The voltage readings on the variac used were checked against the readings given by an amprobe, Model RS-3, AC. Volt. Ammeter, Ohmmeter #D 54599, Pyramid Instrument Corporation, New York.

B. Air leak prevention

To check for air leakage in the system the following approaches were used:

1. An air pressure of seven lb/in² was applied to the system, and it was observed that the pressure decreased rapidly. The reason for this rapid decrease was a leak from the top of the evaporator along the flange. This leak was prevented by using nonhardening Permatex which was applied between the Plexiglas top and the rubber gasket. Although Permatex was used, a slow drop in the pressure applied to the system continued to exist. The remaining leaks proved to be too small for detection by a soap

solution technique.

2. The system was dismantled at the different joints. A vacuum gage was attached to the end of each section, and the vacuum pump was turned on until practically complete vacuum was reached in the section under test. The vacuum pump was then turned off. When the gage showed any increase in pressure more tightening was applied, and the operation was repeated until the applied vacuum remained constant.

This test was repeated for each major section in the system until the system, under high vacuum, proved to be leak proof to air.

C. Plexiglas transmission and incident radiation

The transmissivity of Plexiglas was determined by using an Eppley radiation pyrhelimeter. The energy source was the LM/T40/3 infrared, G. E. Lamp. The lamp was placed at a known distance from the sensitive element of the pyrhelimeter. After placing a piece of the Plexiglas used in the research on top of the pyrhelimeter, the lamp was turned on, and a reading was recorded. Another reading was taken after removing the Plexiglas and keeping the lamp turned on. Each reading was taken after a steady-state had been reached. The transmissivity of the Plexiglas was de-

defined as the ratio of the pyrhelimeter reading with the Plexiglas cover being atop of it, to the pyrhelimeter reading without the Plexiglas cover.

The average incident radiation with the infrared lamp being used at full capacity was also determined with the radiation pyrhelimeter.

D. Operation

The evaporator was warmed up for a short period of time with the infrared lamp operating at a low power input; simultaneously, steam was used to purge the system. Purging with steam replaced the air in the evaporator and prevented "vapor lock" during the actual experimental test. The steam was admitted to the system through the receiving chamber of the condenser. At the end of the purging operation, both the inlet and outlet steam valves were turned off at the same time. The vacuum pump was started, and the condenser cooling water was turned on. The steam in the system was drawn to the condenser and collected in the receiver. When the desired vacuum was established, the valve connecting the water feed column to the evaporator was turned on, and a known quantity of water was admitted to the evaporator. The air blower was turned on, and the in-

frared lamp was used at full capacity. The starting time was recorded, and the level gage in the receiver chamber was marked.

The vacuum in the system was kept constant by using a control valve. The cooling water flow rate was measured.

The temperatures of interest in the system were measured by using thermocouples placed at different locations inside and around the evaporator (see Figure 14). This procedure was repeated at different time intervals until steady-state operation was reached. The steady-state operation was reached when the temperatures measured for the different points in the system were constant for a certain length of time. The water level in the receiver chamber was marked, and the experiment was continued for a certain length of time; this time was called "elapsed steady-state time." The water collected during the elapsed steady-state time was pumped out and weighed. The unevaporated water was weighed at the end of the experiment.

VII. PRESENTATION OF EXPERIMENTAL DATA

Six runs were made, and the data were recorded in Table VII in the Appendix. The data taken from run number three were recorded in detail in Table VIII. The detailed account of the data from run number three illustrates the general method followed in taking the data from the respective runs.

Runs were made at five different pressures inside the evaporator, while the other parameters were held as nearly constant as the characteristics of the apparatus would permit.

Run number one was made when the pressure inside the evaporator was kept constant at two lb/in². Due to excessive heat losses by radiation and convection from the flange, most of the condensation occurred along the upper edges of the evaporator. In run number two the pressure inside the evaporator was five lb/in², and at steady-state the average rate of water condensation inside the evaporator

was about 22 droplets/minute. These droplets always started to form at the very upper edges of the evaporator where the welding seam of the flange was located. Condensation occurred in the form of very small spheres of water. Later, these small droplets would adhere together to form a larger droplet and finally stream down to the water basin. The following runs three, four, and five were made after insulating the flange with glass wool. Runs three and four were duplicate runs; that is, approximately the same conditions existed in both runs. At steady-state the pressure inside the evaporator was 0.46 lb/in^2 in each of the two runs. Runs five and six were made respectively at 0.7 lb/in^2 and 1.28 lb/in^2 pressure inside the evaporator. In runs three, four, five, and six condensation appeared to occur only in the condenser (see Table III). The tabulated results for the amount of heat available for water evaporation in each run, are shown in Table IV. The distribution of the incident radiation on the Plexiglas surface was calculated, and the results are shown in Tables V and VI.

TABLE III

PRESSURE INSIDE THE EVAPORATOR FOR EACH
RUN, AND BASIN WATER TEMPERATURE AT STEADY STATE

Run Number	Total Vacuum Applied Inside the Evaporator (inches H _g)	Pressure Inside the Evaporator (lb/in ²)	Basin water Equilibrium Temperature (°F.)
1	23.45	2.00	126
2	17.36	5.00	141
3	26.60	0.46	78
4	26.60	0.46	78
5	26.13	0.70	90
6	24.86	1.28	110

TABLE IV

HEAT AVAILABLE FOR WATER
EVAPORATION IN THE RESPECTIVE RUNS

Run Number	Heat Available for Water Evaporation (Btu/hr)
1	129.5
2	115.45
3	162.42
4	162.42
5	156.51
6	143.24

TABLE V
ACTUAL HEAT DISTRIBUTION FOR THE
RESPECTIVE RUNS

Run Number	1	2	3*	4*	5	6
Q_k	37.55	44.20	21.02	21.02	24.70	28.54
Q_b	1.66	2.22	0.23	0.23	0.53	0.45
$Q_{3 \rightleftharpoons 2}$	1.77	1.35	1.91	1.91	1.36	1.63
Q_t	110.45	100.12	132.44	132.44	128.18	120.19
Q_r	22.12	26.04	23.30	23.30	24.53	24.75
Q_c	40.40	46.66	40.00	40.00	45.06	44.72
$Q_{1 \rightleftharpoons 2}$	19.52	16.20	27.84	27.84	27.00	21.87
$Q_{\text{refl.}}$	11.83	11.83	11.83	11.83	11.83	11.83
Q_g	21.42	15.23	39.00	39.00	36.22	25.90
Q_u	42.36	44.63	11.60	11.60	8.59	28.62
Q_i (total)	308.50	308.50	308.50	308.50	308.50	308.50

*Duplicate runs.

VIII. DISCUSSION OF RESULTS

A. Heat and mass balances

A heat balance for the evaporator unit was accomplished by using the following assumption and approach.

1. Heat loss by conduction from the basin and the evaporator walls.

The evaporator wall was divided into two sections along its height, and the average temperature of the outside wall was measured for each section; the temperatures of the outer skin of the wall insulation were measured for each section. It was assumed for all the runs that the direction of flow of heat by conduction was at all points radial and perpendicular to the axis of the cylinder. The heat loss by conduction was calculated by using the following equation:

$$Q_k = k_m A_m \frac{\Delta t}{\Delta X} \quad (9)$$

Where,

Q_k = Steady rate of heat transfer by conduction
from the evaporator walls to the surroundings

(Btu/hr).

k_m = Mean thermal conductivity of the insulation
(Btu/hr-ft-°F).

A_m = Logarithmic mean area through which heat flows
at right angles to the insulation surface (ft²).

Δt = Temperature difference across the insulation
(°F.).

Δx = Thickness of insulation (ft).

A_m , Δt , and Δx were measured and k_m was found in the literature (16).

2. Convection losses.

To determine the convection heat transfer coefficient for the flange before insulation, the following procedure was followed:

Using Figure eight on page 468 of Chemical Engineers' Handbook Reference (32), x was defined by the relation,

$$x = L V_{\infty} \rho_{\infty} / \mu$$

Where,

x = Dimensionless abscissa.

L = Length of heat transfer surface, heated length,
(ft).

V_{∞} = Approach velocity of stream (ft/hr).

ρ_{∞} = Density of stream of great depth (lb_m/ft^3).

μ = Absolute viscosity of stream at bulk temperature ($\text{lb}_m/\text{ft-hr}$).

Calculating x , and using the curve denoted by (ELF), j was found. The expression j was defined by the relation,

$$j = (h/C_p V_{\infty} \rho_{\infty}) (C_p \mu/k)^{2/3}$$

Where,

j = Dimensionless ordinate.

h = Local coefficient of heat transfer ($\text{Btu/hr-ft}^2\text{-}^{\circ}\text{F}$).

C_p = Specific heat of stream at constant pressure ($\text{Btu/lb-}^{\circ}\text{F}$).

k = Thermal conductivity of fluid ($\text{Btu/ft-hr-}^{\circ}\text{F}$).

Once j was found, the convection heat transfer coefficient from the bare flange to the surroundings could be determined. The amount of heat lost by convection in the case of a bare flange would be:

$$Q''_c = h A \Delta t \quad (10)$$

Where,

h = Convection heat transfer coefficient from the

bare flange to the surroundings (Btu/hr-ft²-°F).

Q''_c = Rate of heat lost by convection from the bare flange (Btu/hr).

A = Surface area of the exposed flange (ft²).

The heat loss by convection from the Plexiglas top was determined as follows:

To find h_c the equation (Reference (21) page 140),

$$h_c = 0.99 + 0.21 V \quad (4)$$

was used.

Where,

h_c = Convection heat transfer coefficient from the outside Plexiglas surface to the surrounding atmosphere (Btu/hr-ft²-°F).

V = Wind velocity (ft/sec).

Once h_c was found, the rate of heat loss by convection from the Plexiglas was simply found by using equation (10) in the form,

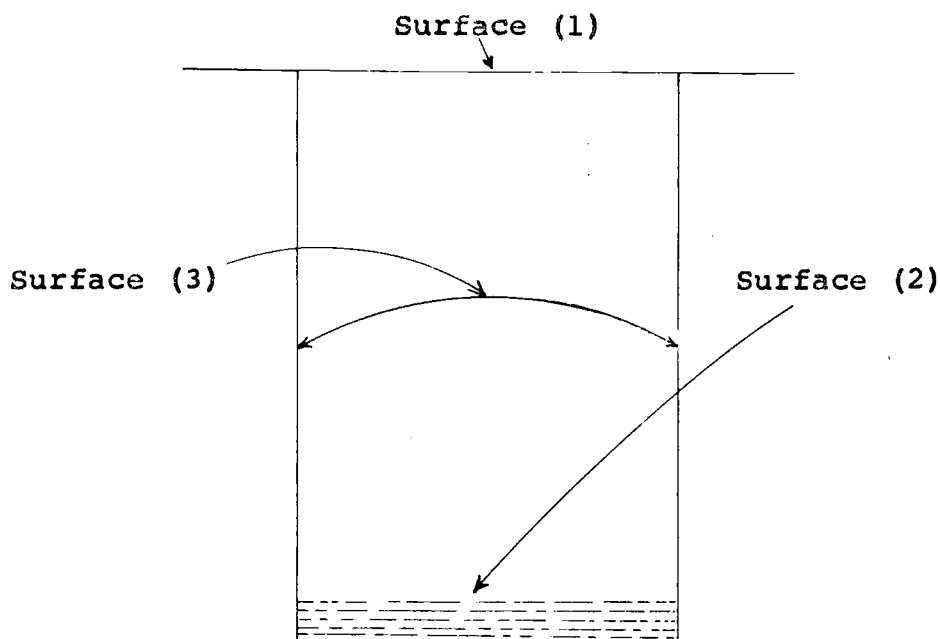
$$Q_c = h_c A \Delta t \quad (11)$$

Where,

Q_c = Rate of heat lost by convection from the Plexiglas surface to the surroundings (Btu/hr).

3. Radiation heat transfer.

In order to make a balance on the radiant energy, the evaporator was divided into three surfaces.



Surface (1) = The underside surface of the Plexiglas.

Surface (2) = Surface of the water in the basin.

Surface (3) = Surface of the evaporator walls.

The following terms were defined:

Q_k = Rate of heat loss by conduction from the evaporator walls (Btu/hr).

Q_b = Rate of heat loss by conduction through the water basin ($\frac{\text{Btu}}{\text{hr}}$).

Q_i = Rate of incident radiation on the Plexiglas cover ($\text{Btu/hr} \cdot 0.785 \text{ ft}^2$).

Q_t = (Rate of available heat for evaporation transmitted through the Plexiglas) + (Rate of heat gain to the water basin by conduction from the evaporator walls), (Btu/hr).

Q' = Rate of heat loss to the walls by convection from the heat transmitted to the inside of the evaporator (Btu/hr).

$Q_{1 \rightleftarrows 3}$ = Net rate of radiation heat interchange between surfaces (1) and (3), (Btu/hr).

$Q_{1 \rightleftarrows 2}$ = Net rate of radiation heat interchange between surfaces (1) and (2), (Btu/hr).

$Q_{3 \rightleftarrows 2}$ = Net rate of radiation heat interchange between surfaces (3) and (2), (Btu/hr).

$Q_{\text{refl.}}$ = Rate of heat reflected from the outside surface of the Plexiglas cover (Btu/hr).

Q_r = Net radiation interchange between the Plexiglas cover and the surrounding atmosphere (Btu/hr).

The following equation may be written:

$$Q_k = Q' + Q_{1 \rightleftarrows 3} - Q_{3 \rightleftarrows 2} \quad (12)$$

To find $Q_{1 \rightleftarrows 3}$ consider the view factor relationships: the black-surface over-all interchange factor \bar{F}_{12} is defined as the fraction of the radiation leaving black surface A_1 in all directions which reaches and is absorbed by surface A_2 , directly and by aid of reflection and/or re-radiation.

Where,

$$A_1 = \text{Area of surface (1) (ft}^2\text{)}.$$

$$A_2 = \text{Area of surface (2) (ft}^2\text{)}.$$

The equations for the interchange factors can be written as

$$\bar{F}_{12} = \bar{F}_{21} \quad (13)$$

$$\bar{F}_{13} = \bar{F}_{23} \quad (14)$$

Since,

$$A_1 \bar{F}_{12} = A_2 \bar{F}_{21} \text{ and } A_1 \bar{F}_{13} = A_2 \bar{F}_{23}$$

and since,

$$A_1 = A_2$$

also,

$$\bar{F}_{12} + \bar{F}_{13} = 1 \quad (15)$$

The interchange factor \bar{F}_{12} was found from Reference (22) and \bar{F}_{13} was found from equation (15). Assuming a gray enclosure,

$Q_{1 \rightleftarrows 3}$ was found by the equation:

$$Q_{1 \rightleftarrows 3} = A_1 \mathcal{F}_{13} \sigma (T_1^4 - T_3^4) \quad (16)$$

Where,

A_1 = Area of surface (1).

\mathcal{F}_{13} = Overall interchange factor, representing the radiation reaching surface A_3 due to original emission from A_1 only, but including assistance given by reflection at other source - sinks.

σ = Stefan-Boltzmann constant = 0.1713×10^{-8}
(Btu/ft²-hr-(°R)⁴).

T_1 = Absolute temperature of surface (1), (°R).

T_2 = Absolute temperature of surface (2), (°R).

\mathcal{F}_{13} was found by the equation:

$$\frac{1}{A_1 \mathcal{F}_{13}} = \frac{1}{A_1} \left(\frac{1}{\epsilon_1} - 1 \right) + \frac{1}{A_3} \left(\frac{1}{\epsilon_3} - 1 \right) + \frac{1}{A_1 \mathcal{F}_{13}} \quad (17)$$

Where,

A_1 and A_3 = Respectively, the areas of surfaces
(1) and (3), (ft²).

ϵ_1 = Emissivity of surface 1.

ϵ_3 = Emissivity of surface 3.

Emissivity is defined as the ratio of the actual

emissive power of a surface at a given temperature to the emissive power of a black body at the same temperature. Emissivity values were found in the literature (22, 32) and when normal emissivity was reported, it was corrected to give total hemispherical emissivity.

$Q_{1\leftrightarrow 2}$ is found in a procedure similar to that used to find $Q_{1\leftrightarrow 3}$. When Q' was found from Equation (12), Q_t will be:

$$Q_t = Q_s - Q' \quad (18)$$

Where,

Q_s = Rate of radiation transmitted through the Plexiglas cover (Btu/hr).

Since the transmissivity of the Plexiglas was determined experimentally, Q_s will be:

$$Q_s = \tau Q_i \quad (19)$$

Where,

τ = Transmissivity.

The amount of heat, reflected from the Plexiglas surface is:

$$Q_{\text{refl.}} = \rho Q_i \quad (20)$$

ρ = Plexiglas reflectivity.

The relation between τ , ρ , and the Plexiglas absorptivity is:

$$\rho + \alpha + \tau = 1 \quad (21)$$

Where,

α = Absorptivity of Plexiglas.

Finally, the incident radiation, at the Plexiglas cover, was balanced against the respective values for the heat distribution.

$$Q_i = Q_k + Q_{3 \rightleftarrows 2} + Q_t + Q_r + Q_c + Q_{1 \rightleftarrows 2} + Q_{\text{refl.}} + Q_u + Q_g \quad (22)$$

Where,

Q_u = Rate of heat losses due to vapor absorption by radiation, and other unaccounted for heat losses, (Btu/hr).

Q_g = Rate of heat transferred to the vapors passing along the underside of the Plexiglas surface (Btu/hr).

The heat available for water evaporation was approximately:

$$Q_A = Q_{1 \rightleftarrows 2} + Q_t + Q_{3 \rightleftarrows 2} + Q_b \quad (23)$$

Where,

Q_A = Rate of heat available for evaporation (Btu/hr).

Q_b , is positive when it is a gain from the surroundings to the basin of water and negative when it is a loss from the basin of water to the surroundings, (Btu/hr). The rate of water evaporated and collected was checked against the amount of heat available for evaporation.

A full analysis of the results obtained from these calculations is shown in the following section.

B. Analysis of results.

The heat available for water evaporation increased with a decrease in the pressure applied inside the evaporator. This relationship is shown in Figure sixteen and Table IV. It was not possible to check the amount of heat available in the first and second runs against the weight of water evaporated and collected because condensation in these two runs occurred at the upper edge of the evaporator, where heat losses by convection and radiation from the flange were high. In the following runs, the flange was insulated and since lower pressures were applied inside the evaporator, condensation occurred in the condenser and none in the evaporator. Table III shows the pressure inside the evaporator and the basin water equilibrium temperature in each run. The accuracy of basin temperature determinations was checked and

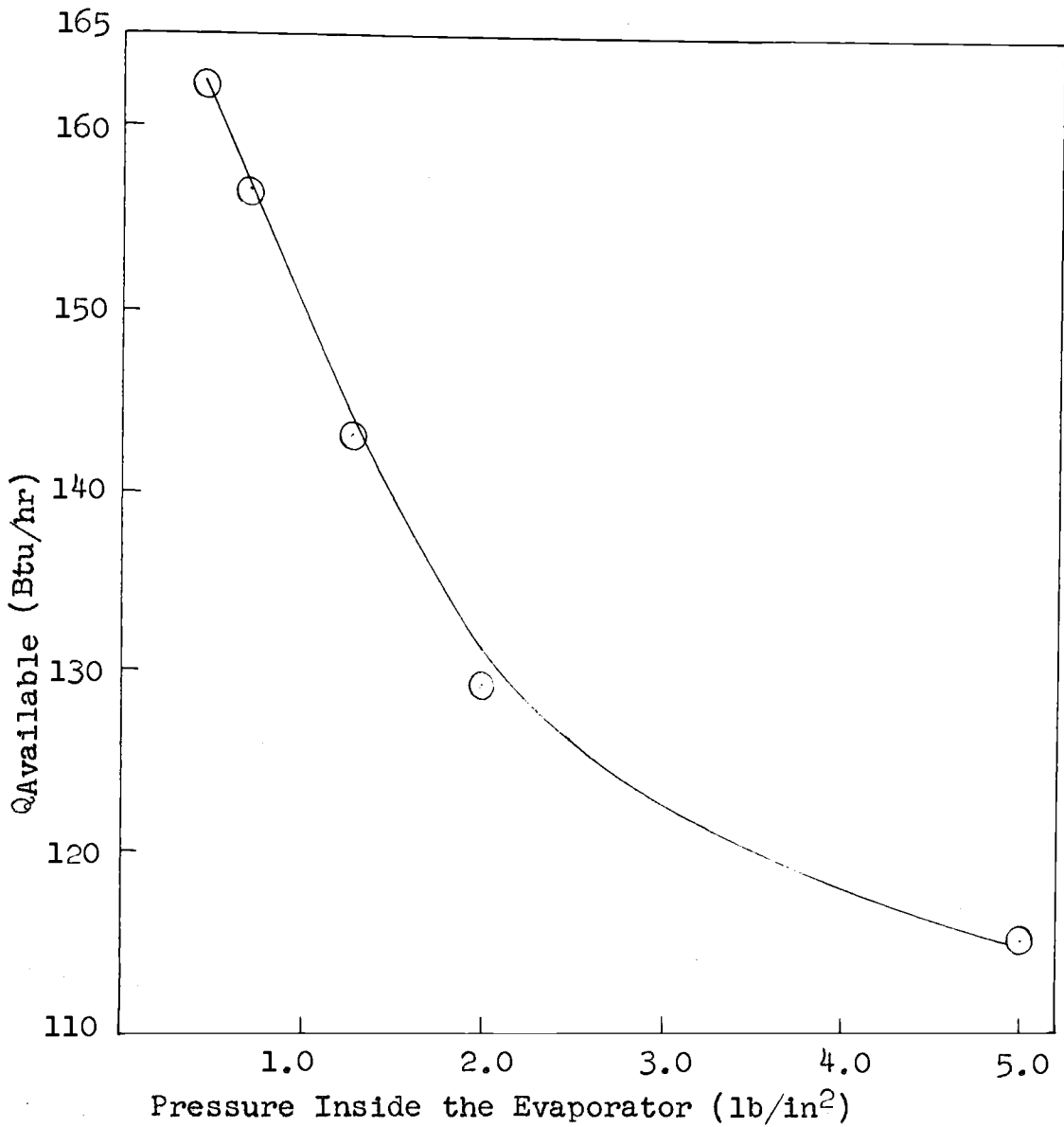


Figure 16: Heat Available for Water Evaporation
Versus Pressure Applied Inside the
Evaporator.

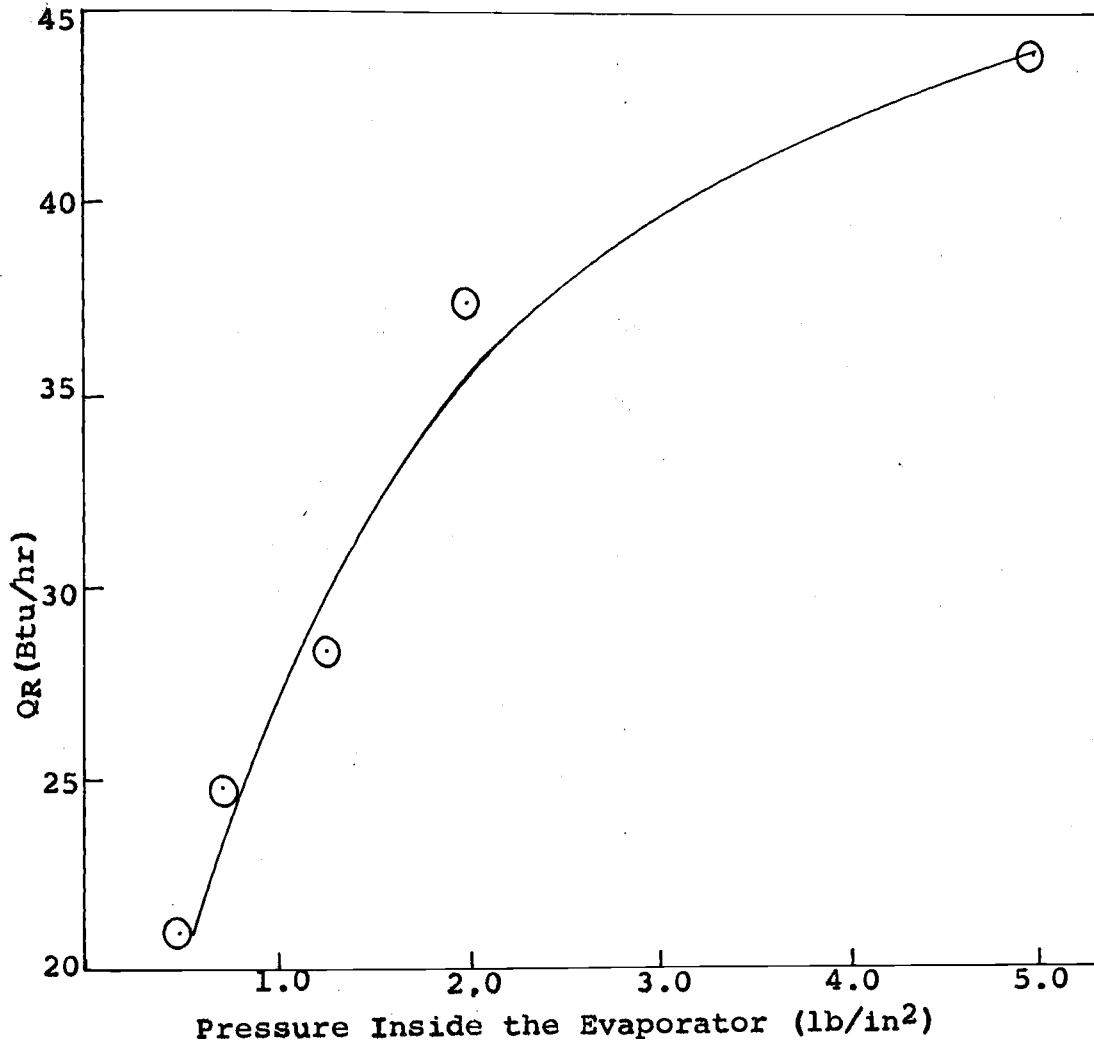


Figure 17: Rate of Heat Loss by Conduction Through the Walls as a Function of the Pressure Inside the Evaporator.

proved to be very satisfactory. For example, under a pressure of two lb/in² absolute, the temperature of saturated steam is 126.08°F. (32), and the reported basin temperature by thermocouple number zero was 126°F. Thus the reliability of the calibration of thermocouples was established and thermocouple temperature measurements were considered to be fairly accurate. In run number three the rate of water evaporated and collected at steady state was 72 g/hr. This value checks well with the amount of water which could have resulted from the calculated heat available for water evaporation. The per cent deviation was 2.6%. The per cent deviation, between the weight of water evaporated and collected in each of the two runs three and four was 4.64%. The difference between the experimental and calculated values could be attributed to minor changes in the applied conditions and to visual error in determining the water level.

The actual and per cent heat distribution is shown respectively in Tables V and VI. The heat loss due to absorption by the vapor and other unaccounted for heat losses were 3.61, 2.96, and 9.4 per cent respectively in runs number four, five, and six.

The rate of water evaporated and collected from the condenser chamber increased as expected with a decrease in the pressure applied inside the evaporator; this is shown in Figure 18.

Figure 19 shows the equilibrium basin temperatures as a function of the applied pressure inside the system. When the pressure was five lb/in², the maximum attainable temperature by the water basin was approximately 141° F., while the boiling point of water under the given pressure is about 162° F. This behavior was due directly to the high rate of heat loss by convection and radiation from the Plexiglas cover. Since the Plexiglas transmissivity was 43.8 per cent for the infrared lamp used, these high losses were expected. It should be noted that the transmissivity of Plexiglas for solar energy is 85 per cent as determined in the Solar Laboratory of the University of Arizona.

As it appears in Table VIII, the evaporator wall temperature decreased with an increase in the distance between the lamp and a point on the wall.

The incident radiation at the Plexiglas surface was measured accurately by a standardized radiation pyrhelio-
meter. The pressure inside the vessel was measured with a

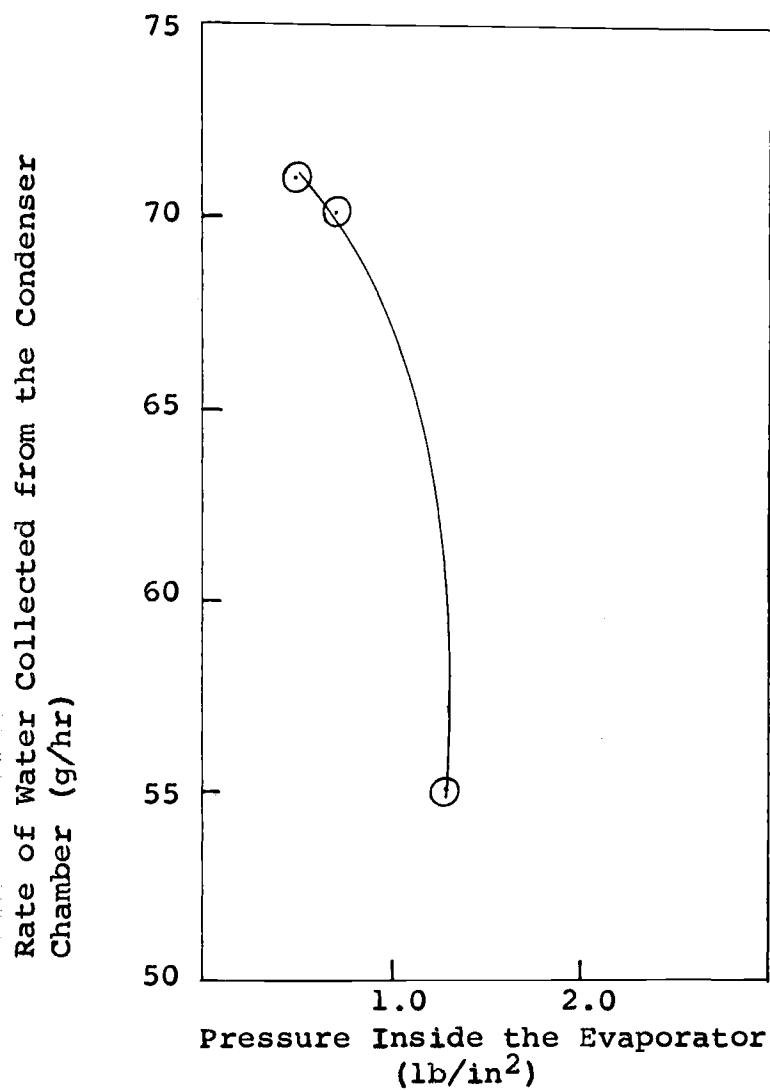


Figure 18: Rate of Water Collected from the Condenser Chamber as a Function of the Applied Pressure Inside the Evaporator.

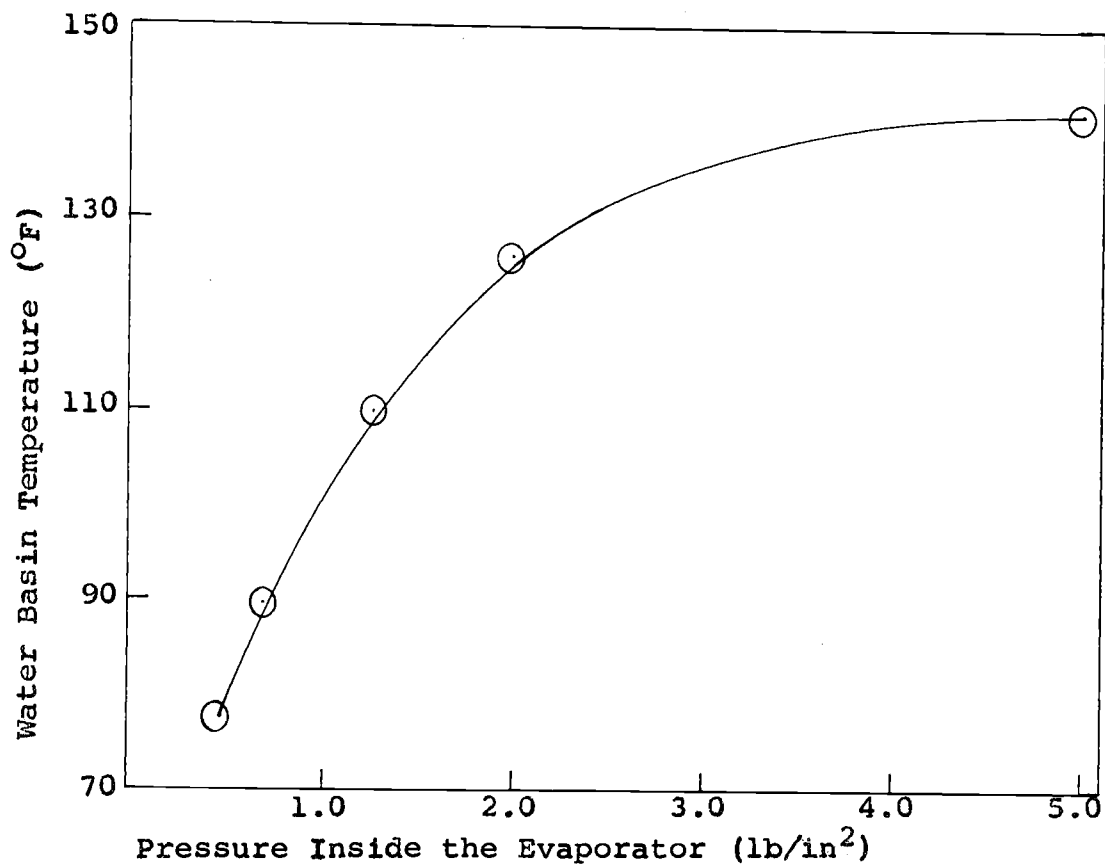


Figure 19: Water Basin Temperature as a Function
of the Pressure Applied Inside the
Evaporator.

mercury manometer. The barometric reading was used to correct this value obtained from the manometer.

Finally, it should be noted that conduction losses would have been greatly reduced if the walls of the evaporator had not been as long and if the evaporator had been made of concrete. If salt water were used in this experiment it would be expected not to have any significant scale formation when the system was used at high vacuum. This prediction was mainly due to the inverted solubility curve of calcium sulfate, which was a major scale forming in desalination processes using distillation.

It should be noted further that the net radiation always occurred from the cover to the basin, and this would hold true if solar energy were used and low pressure were applied to the system.

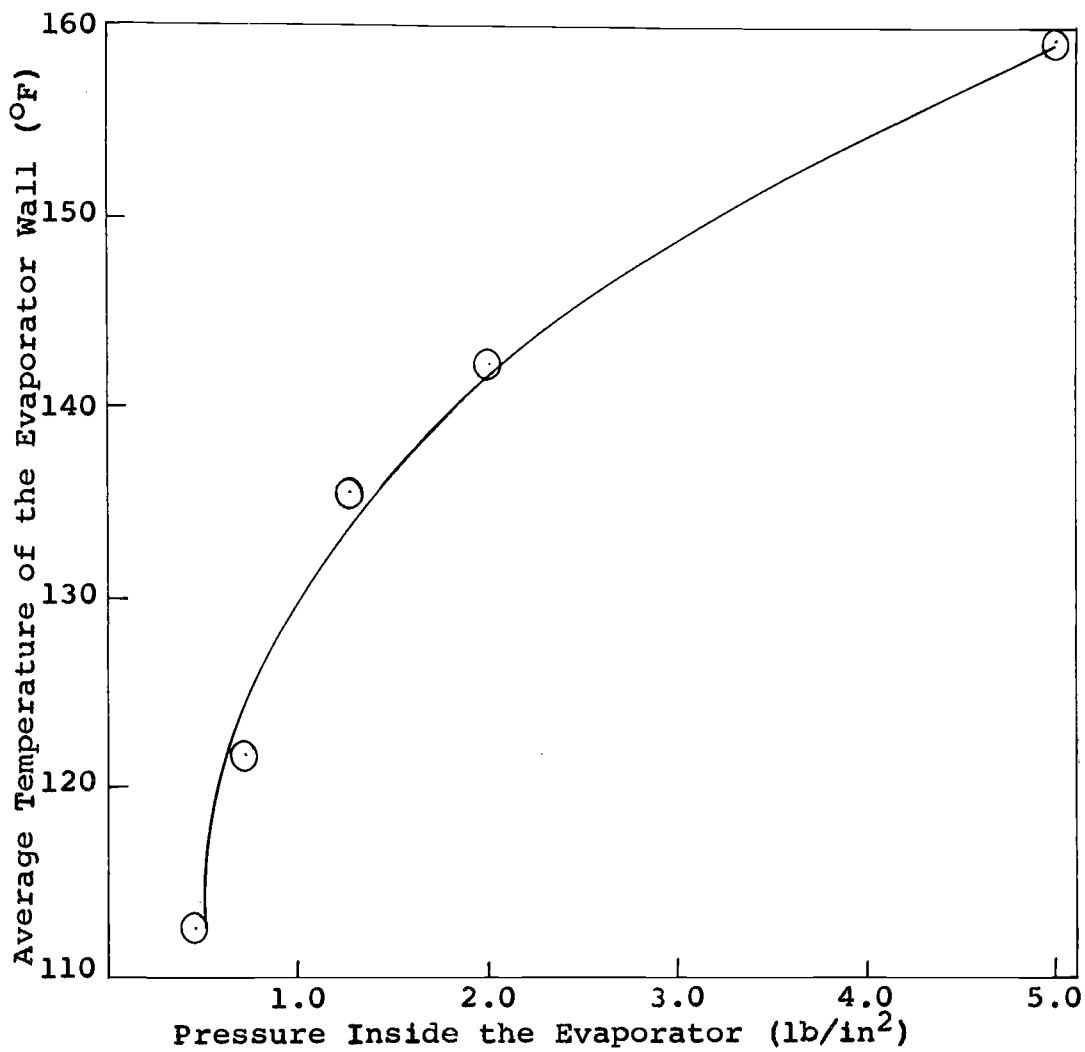


Figure 20: Average Wall Temperature of the Evaporator as a Function of the Pressure Inside the Evaporator.

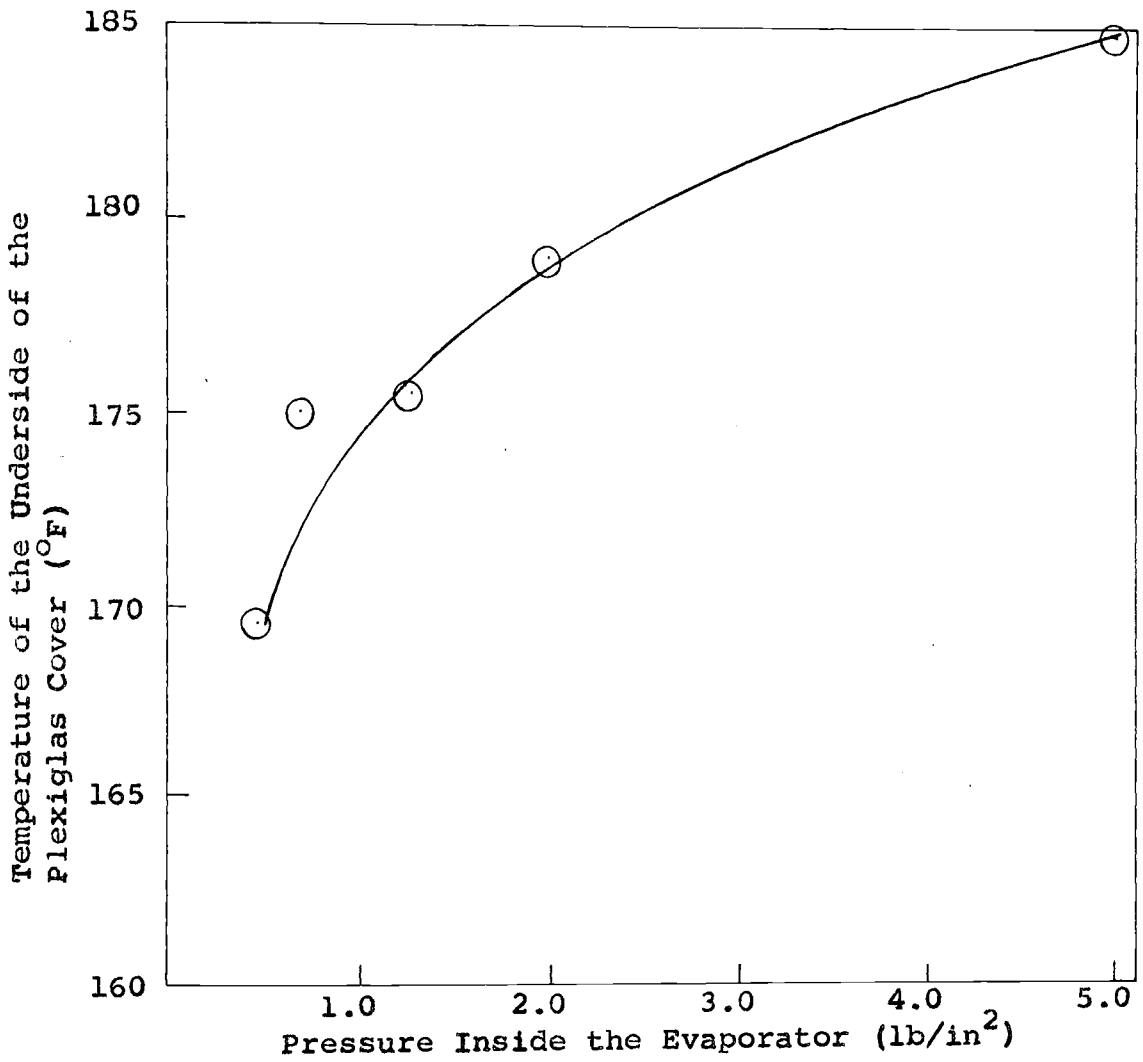


Figure 21: Temperature of the Underside of the Plexiglas Cover Versus the Pressure Inside the Evaporator.

IX. SUMMARY

This research was a preliminary study of the possibility of developing a new process for saline water conversion, using vacuum and the low temperatures in a cooling tower. The low temperatures in a cooling tower were needed to furnish the cooling water necessary for vapor condensation when evaporation would occur under high vacuum. The experimental data showed a sensible increase in the rate of water evaporated when the pressure in the system was decreased. The theoretical accounting for the heat available for water evaporation, checked satisfactorily with the weight of water evaporated and collected.

Radiation losses from basin to cover, which usually occur in conventional solar stills, did not exist under the conditions of this research. In fact the net radiation always occurred from the cover to the basin. Under the principle used, convection losses were nonexistent, and the sensible heat necessary to bring the water basin to equil-

ibrium was less than that of the regular solar stills.

Under the temperatures prevailing in low vacuum, oxidation and scale formation were almost entirely prevented.

X. RECOMMENDATIONS

Since this work represents a preliminary step toward the major research project of economical conversion of sea water using vacuum and solar energy, the following recommendations are made:

1. Further study of the basic principle of the process by investigating the productivity of the still when it is used under the sun in a desert site.
2. The walls of the desert unit should be made of concrete and the distance between the still cover and the basin should be kept to a minimum.
3. A plate glass cover should be used, instead of Plexiglas. Glass is more durable and its surface does not scratch as easily as Plexiglas.

These recommendations are based on the experimental data and the calculated desert cases which all proved that the solar vacuum technique is promising and should be fur-

ther investigated.

XI. ACKNOWLEDGEMENTS

The author wishes to express his sincere appreciation to Dr. Donald H. White, the director of this study, whose patient guidance, encouragement, and inspiration were invaluable.

I am greatly indebted to Mr. Richard M. Edwards and Mr. Thomas Breen for their assistance in the building of the equipment and particularly for their patience with me. Sincere thanks are due to Professors: Neil D. Cox, Raymond C. Richardson, and Edward J. Freeh for their support, advice, and constructive criticism.

The appreciation of the author to his wife Shirley Ann for her encouragement, hard work, and the typing of this thesis is beyond expression.

XII. LITERATURE CITED

1. American Chemical Society, Advances In Chemistry Series #27, "Saline Water Conversion", Washington, D. C. (1960).
2. Association for Applied Solar Energy-Stanford Research Institute, Proceedings of the "World Symposium on Applied Solar Energy", Phoenix, Arizona (November 1-5, 1955), Jorgenson & Company, San Francisco, California.
3. Bird, R. B., W. E., Stewart, and E. N. Lightfoot, "Transport Phenomena", John Wiley and Sons, Inc., New York, London, 2nd Printing (January, 1961).
4. Bixler, G. H., Saline Water Conversion: How it's progressing, where it's heading, "J. Chemical and Engineering News", Vol. 41 #23 pp. 46-52 (June 10, 1963).
5. Brown, G. G., "Unit Operations", John Wiley and Sons Inc., New York (1950).
6. Brownell, L. E., and E. H. Young, "Process Equipment Design", John Wiley and Sons, Inc., New York, Chapman and Hall Limited, London (1959).
7. Cadwallader, E. A., "Ind. and Engineering Chem.", Vol. 54 #3, pp. 26-33 (March, 1962).
8. Centre Nationale De La Recherche Scientifique, "Applications Thermiques De L'Energy Solarie Dans Le Domaine De La Recherche Et De L'industrie", Colloques Internationaux Du Centre Nationale De La Recherche Scientifique, #LXXXV, Mont Louis 23-28 June 1958, 15, Quai Anatole, France, Paris (VII^e), (1961).
9. Clarke, L., "Manuel for Process Engineering Calculations", McGraw-Hill Book Co., Inc., New York and London, 1st Edition (1947).

10. Corning Glass Works, "Properties of Selected Commercial Glasses", Corning, New York (April 1961).
11. Daniels, F., and J. A. Duffey, eds., "Solar Energy Research", University of Wisconsin Press, Madison, (1955).
12. Faust, R. J., Desalinization and Future Water Supply in the United States, "Journal American Water Works Association", Vol. 54 #5, pp. 519-525 (May 1962).
13. Hodges, C. N., and Richard Kassander Jr., "Distillation of Saline Water Utilizing Solar Energy", in a multiple effect system consisting of separate Collector, Evaporator, and Condenser; Introductory Report, The University of Arizona, Solar Energy Laboratory of the Institute of Atmospheric Physics (April 1, 1962).
14. Hodgman, C. D., "Handbook of Chemistry and Physics", Chemical Rubber Publishing Co., Cleveland, Ohio, 39th Edition (1958).
15. Jenkins, D. S., Director, "A Standardized Procedure for Estimating Costs of Saline Water Conversion:", office of Saline Water, U. S. Dept. of the Interior (March, 1956).
16. Johns - Manville, "Industrial Insulations Catalog", Copyright by Johns-Manville Corp., (1959).
17. Ketola, N. H., "The Application of Thermoelectric Energy Conversion to the Design of a Saline Water Distillation Unit", Thesis, The University of Arizona Library (1961).
18. Kutchinski, H. P. Jr., "Performance of a Flat-Plate Solar Energy Collector Using a Low-Emissivity Glass Cover", Thesis, The University of Arizona Library (1961).
19. Loebel, F. A., "Brackish Water Conversion in the United States", paper presented at the Desalination Research Conference (June 22, 1961), Woods Hole,

Massachusetts (June 19-July 14, 1961), Aqua-Chem. Inc., Waukesha, Wisconsin.

20. Maron, S. H., and C. F. Prutton, "Principles of Physical Chemistry", The Macmillan Co., New York, 2nd Printing (1959).
21. Mason, M. A., Office of Saline Water, U. S. Dept. of the Interior, "Symposium on Saline Water Conversion", proceedings of a symposium, 4-6 November 1957, publication 568, Washington, D. C. (1958).
22. Mcadams, W. H., "Heat Transmission", McGraw-Hill Book Co., Inc., New York, Toronto, London, 3rd Edition (1954).
23. McCabe, W. L., and J. C. Smith, "Unit Operation of Chemical Engineering", McGraw-Hill Book Co., Inc., New York, Toronto, London (1956).
24. Merriman, T., and T. H. Wiggin, "Civil Engineers' Handbook", John Wiley and Sons, Inc., New York, Chapman and Hall Ltd., London, 5th Edition (1950).
25. Office of Saline Water, U. S. Dept. of the Interior, "Third Annual Report of the Secretary of the Interior", on Saline water conversion, Washington 25, D. C. (January 1955).
26. Office of Saline Water, U. S. Dept. of the Interior, "Saline Water Conversion Report for 1960", Washington 25, D. C. (January 1961).
27. Office of Saline Water, U. S. Dept. of the Interior, "Saline Water Conversion Report for 1961", Washington 25, D. C. (January 1962).
28. Office of Saline Water, U. S. Dept. of the Interior, "Desalination Research and the Water Problem", Report of the Desalination Research Conference convened by the NAS-NRC, at Woods Hole, Massachusetts June 19-July 14, 1961, Publication 941, Washington, D. C. (1963).

29. Office of Saline Water, U. S. Dept. of the Interior and The National Science Foundation, "Desalination Research Conference", Proceedings of the Conference on Desalination Research, organized and convened by the NAS-NRC, at Woods Hole, Massachusetts June 19-July 14, 1961, Publication 942, Washington, D. C. (1963).
30. Office of Saline Water, U. S. Dept. of the Interior, "Saline Water Conversion", A Program to develop a new source of fresh water, Superintendent of Documents, U. S. Government printing office, Washington 25, D. C. (1962).
31. Office of Saline Water, U. S. Dept. of the Interior, "Saline Water Conversion Report for 1962", Washington 25, D. C. (January 1962).
32. Perry, J. H., "Chemical Engineers' Handbook", McGraw-Hill Book Co., New York, 3rd Edition (1950).
33. Spiegler, K. S., "Salt Water Purification", John Wiley and Sons, Inc., New York, London (1962).
34. Staley, K. A., "Fundamentals of Light and Lighting", Large Lamp Dept., General Electric Co., Bulletin LD-2, (August, 1960).
35. Telkes, M., Fresh Water from Sea Water by Distillation, "J. Industrial and Engineering Chemistry", Vol. 45 #5, pp. 1108-1114 (May, 1953).
36. Urquhart, Leonard, Church, "Civil Engineering Handbook", McGraw-Hill Book Co., Inc., New York, Toronto, London, 1st Edition (1950).
37. Zaitsev, D. V., "Demineralization of Water (1948)", A translation from the Russian, for the office of Saline Water, U. S. Dept. of the Interior; gift from Shneiderov, A. J., (April 17, 1958).

XIII. APPENDIX

TABLE VII

DATA FROM TEST RUNS AT STEADY-STATE

Run	1	2	3
Date	8/9/63	8/12/63	8/13/63
Time of Start	12 noon	8:45 AM	9:15 AM
Room Temperature ($^{\circ}\text{F.}$)	79	80	82
Atm. Pressure (in. H_g)	27.52	27.51	27.54
Wt. of Water Feed (g)	1180	1180	1180
Total Time of Run (minutes)	385	346	300
Total Vacuum Inside System (in. H_g)	23.45	17.36	26.6
Wind Velocity on Top of Plex. Surface (mph)	1.5	1.5	1.5
Steady-State Time (minutes)	135	46	90
Wt. of water evaporated & collected in Condenser Chamber Corresponding to Steady State Time (g)	25.9	5.2	108
Temp. of the Outside Surface of Plexiglas Cover ($^{\circ}\text{F.}$)	119	121	116
Temp. of the Underside of Plexiglas Cover ($^{\circ}\text{F.}$)	179	185	169.5
Ave. Flange Surface Temp. ($^{\circ}\text{F.}$)	99	98.5	96
Temp. of Flange Insulation Outer Skin ($^{\circ}\text{F.}$)	--	--	86
Basin Water Temperature ($^{\circ}\text{F.}$)	126	141	78
Temp. From Thermocouple No. 1 ($^{\circ}\text{F.}$)	130	149	88
Temp. From Thermocouple No. 2 ($^{\circ}\text{F.}$)	144	162	114
Temp. From Thermocouple No. 3 ($^{\circ}\text{F.}$)	153	165	135
Temp. From Thermocouple No. 4 ($^{\circ}\text{F.}$)	93	95.5	85.5
Temp. From Thermocouple No. 5 ($^{\circ}\text{F.}$)	95	98	87.5
Temp. From Thermocouple No. 6 ($^{\circ}\text{F.}$)	99.5	102	94
Temp. From Thermocouple No. 7 ($^{\circ}\text{F.}$)	111	122	79
Temp. From Thermoc. No. 8 ($^{\circ}\text{F.}$)	89	92.5	82

TABLE VII
(Continued)
DATA FROM TEST RUNS AT STEADY-STATE

Run	4	5	6
Date	8/13/63	8/14/63	8/14/63
Time of Start	7:00 PM	10:30 AM	6:40 PM
Room Temperature (°F.)	81	81	81
Atm. Pressure (in. H _g)	27.48	27.55	27.46
Wt. of Water Feed (g)	1180	1180	1180
Total Time of Run (minutes)	185	302	192
Total Vacuum Inside System (in. H _g)	26.54	26.13	24.86
Wind Velocity on Top of Plex. Surface (mph)	1.5	1.5	1.5
Steady-State Time (minutes)	40	72	30
Wt. of water evaporated & collected in Condenser Chamber Corresponding to Steady-State Time (g)	50.5	84.6	27.5
Temp. of the Outside Surface of Plexiglas Cover (°F.)	115.7	119.7	120.3
Temp. of the Underside of Plexiglas Cover (°F.)	169.5	175	175.5
Ave. Flange Surface Temp. (°F.)	97	97	100
Temp. of Flange Insulation Outer Skin (°F.)	86	85	91
Basin Water Temperature (°F.)	78	90	110
Temp. From Thermocouple No. 1 (°F.)	88	99.5	118
Temp. From Thermocouple No. 2 (°F.)	114.5	123	138
Temp. From Thermocouple No. 3 (°F.)	135	141.5	148.5
Temp. From Thermocouple No. 4 (°F.)	85.5	89	91.5
Temp. From Thermocouple No. 5 (°F.)	87.5	91	95
Temp. From Thermocouple No. 6 (°F.)	94	98	100

TABLE VII
(Continued)DATA FROM TEST RUNS AT STEADY-STATE

Run	4	5	6
Temp. From Thermocouple No. 7 (°F.)	79	93	105
Temp. From Thermocouple No. 8 (°F.)	82	86	99

TABLE VIII

DATA FROM RUN NUMBER 3

Date	August 13, 1963
Time of Start	9:15 AM
Room Temp. ($^{\circ}$ F.)	82
Atmospheric Pressure (in. H _g)	27.54
Wt. of Water feed (g)	1180
Total time of run (minutes)	300
Total Vacuum inside the system (in. H _g)	26.6
Wind velocity on top of the Plexiglas surface (mph)	1.5
Steady-State time (minutes)	90
Wt. of Water Evaporated and collected in the Condenser Chamber corresponding to steady state time (g)	108

Water Flow Rate Through The Condenser

Time Elapsed (min.)	lb/min.
0	28
19	26.5
212	23.5
297	20.0

TABLE VIII
(Continued)

Cooling Water Temperatures at Inlet and Outlet

<u>Inlet to Condenser</u>		<u>Outlet from Condenser</u>	
Time Elapsed (minutes)	Temperature (°F.)	Time Elapsed (minutes)	Temperature (°F.)
0	80.5	8	81.4
7	80.9	32	81.1
33	80.5	214	82.9
213	82.3	292	83.1

Temperature of Outside Surface of Plexiglas Top

<u>Center</u>		<u>3" from Center</u>		<u>6" from Center</u>	
T. Elapsed (minutes)	Temp. (°F.)	T. Elapsed (minutes)	Temp. (°F.)	T. Elapsed (minutes)	Temp. (°F.)
2	105	2½	105	2½	100
22	111	22½	111	23	105
73	121	73½	118	74	106
104	121	104½	118	105	106
203	122	203½	119	204	106
215	122	215½	119	216	106
293½	122	294	119	294½	106

Exposed Flange Temperatures

<u>Temp. of Flange Surface</u>		<u>Temp. of Insulation Outer Skin</u>	
Time Elapsed (minutes)	Temperature (°F.)	Time Elapsed (minutes)	Temperature (°F.)
9½	90	8½	85
26	91	26½	86
78	92	77	86
706	97	205	86
218	97	217	86
293	97	298½	86

TABLE VIII
(Continued)

<u>Basin Water Temperature</u>		<u>Underside Temp. of Plexiglas Cover</u>	
<u>Time Elapsed (minutes)</u>	<u>Temperature (°F.)</u>	<u>Time Elapsed (minutes)</u>	<u>Temperature (°F.)</u>
0	82	0	137
4	82	3½	140
13	80	13½	150
38	78	40	160
63	78	64	163
75	78	76	163
80½	78	81	163
130½	78	95	165
162	78	102	166
222	78	123	167
283	78	127	168
		157½	168
		162	169
		173	169.5
		187	169.5
		207	169.5
		223	169.5
		283	169.5

TABLE VIII
(Continued)

<u>Thermocouple No. 1</u>		<u>Thermocouple No. 2</u>		<u>Thermocouple No. 3</u>	
T. Elapsed (minutes)	Temp. (°F.)	T. Elapsed (minutes)	Temp. (°F.)	T. Elapsed (minutes)	Temp. (°F.)
14½	87	15	101	15½	109
31½	87	32	105	32½	119
81½	87	82	109	82½	126
131½	88	132	112	133	132
189	88	189½	114	190	135
225	88	225½	114	226	135
284	88	284½	114	285	135
<u>Thermocouple No. 4</u>		<u>Thermocouple No. 5</u>		<u>Thermocouple No. 6</u>	
T. Elapsed (minutes)	Temp. (°F.)	T. Elapsed (minutes)	Temp. (°F.)	T. Elapsed (minutes)	Temp. (°F.)
16	84	16½	85	17	89
33	85	33½	86	34	90
83	85	83½	87	84	92
134	85	134½	87	135	93.5
191	85.5	197	87.5	198	94
226½	85.5	227	87.5	227½	94
285½	85.5	286	87.5	286	94
<u>Thermocouple No. 7</u>		<u>Thermocouple No. 8</u>			
T. Elapsed (minutes)	Temp. (°F.)	T. Elapsed (minutes)	Temp. (°F.)		
17½	79.3	18	82.5		
34½	79	35	82		
84½	79	85	82		
135½	79	136	82		
228	79	228½	82		
287	79	288	82		

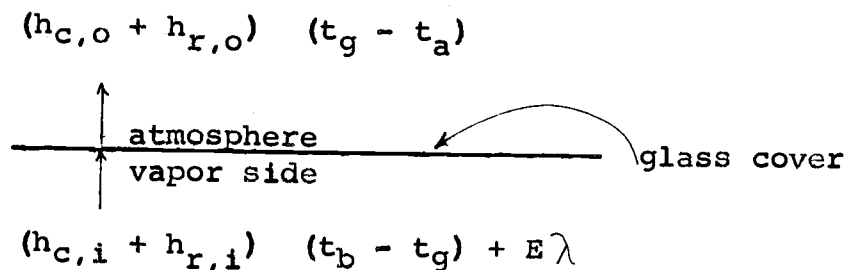
GENERAL APPROACH FOR HEAT AND MASS BALANCE AROUND A

REGULAR DEEP BASIN SOLAR STILL

The following is assumed:

1. A glass covered distiller is used.
2. Total productivity of the distiller each month is the monthly average as determined by use of mean values of solar radiation and atmospheric temperatures.
3. Absorption in the transparent cover, and temperature drop across the two surfaces of the cover are neglected.
4. Assume a period of 24 hour operation.
5. The cover area is equal to the basin area.
6. The brine effluent rate is equal to the distillate rate.
7. Sea water is preheated to distillate temperature.
8. Effective sky temperature for radiation is equal to atmospheric temperature.
9. Conduction heat losses from the basin to the surroundings are $50 \text{ Btu/ft}^2\text{-day}$.

A heat balance around the transparent cover, based on one square foot of cover area gives:



or,

$$(h_{c,o} + h_{r,o}) (t_g - t_a) = (h_{c,i} + h_{r,i}) (t_b - t_g) + E\lambda \quad (24)$$

Where,

$h_{c,o}$ = Convection heat transfer coefficient from cover to atm. (Btu/hr-ft²-°F).

$h_{r,o}$ = Radiation heat transfer coefficient from cover to atm. (Btu/hr-ft²-°F).

t_g = Temperature of transparent cover assumed equal to distillate temperature (°F).

t_a = Atmospheric temperature (°F).

t_b = Temperature of salt water in basin (°F).

E = Water evaporation and condensation rate (lb/ft²-hr).

λ = Latent heat of condensation at basin temperature (+ difference in sensible heat of condensate at basin and cover temperatures) approximately = 1050 (Btu/lb).

$h_{c,i}$ = Coefficient of convection heat transfer from salt water surface to cover of still (Btu/hr-ft²-°F).

$h_{r,i}$ = Radiation heat transfer coefficient, from salt surface to cover of still (Btu/hr-ft²-°F).

Reference temperature = t_g (1)

Overall Energy Balance:

Q_{sh} = Net solar radiation absorbed on basin bottom, (Btu/ft²) = (incident radiation - [reflection from cover + reflection from salt water surface + reflection from basin bottom.]

Basis: one hour:

$$\frac{Q_{sh}}{24} = (h_{c,o} + h_{r,o}) (t_g - t_a) + E(t_b - t_g) + L \quad (25)$$

L = Net miscellaneous heat loss: (Btu/hr-ft²).

$E(t_b - t_g)$ = Sensible heat of condensate.

$\left(\frac{W_{da}}{W_{H_2O}} H_{a,b} - \frac{W_{da}}{W_{H_2O}} H_{a,g} \right) E$ = Heat transfer by convection from salt water surface to the cover of the still (Btu).

W_{da} = lb dry air circulating inside the still/hr.

W_{H_2O} = lb H₂O distilled/hr.

$H_{a,b}$ = Enthalpy of dry air at basin temperature (Btu/lb).

$H_{a,g}$ = Enthalpy of dry air at cover temperature (Btu/lb).

Assuming saturation at basin and cover surfaces the following equation was concluded:

$$E = \frac{h_{c,i}(t_b - t_g)}{\frac{W_{da}}{W_{H_2O}} (H_{a,b} - H_{a,g})} \quad (26)$$

E is a function of t_b and t_g .

Substitute E in Equations (24) and (25), solve for t_b and t_g and then solve for (E) using Equation (26). Solve for the unknowns in Equation (24).

$$h_{c,o} = 0.99 + 0.21 V \quad (\text{under practical conditions subject to wind}) \quad (4)$$

V = wind velocity, ft/sec, (reference (21) page 140).

$h_{r,o}$ = is found by using the Stefan-Boltzmann Law:

$$q = \sigma \epsilon T^4 \quad (27)$$

$$q = \frac{\text{Total radiant energy}}{(\text{Unit area}) (\text{Unit time})} = (\text{Btu/ft}^2\text{-hr})$$

Where,

$$\sigma = \text{Stefan-Boltzmann constant} = 0.1713 \times 10^{-8} \quad (\text{Btu/ft}^2\text{-hr-(}^\circ\text{R)}^4).$$

ϵ = Emissivity of the glass cover.

$$h_{r,o} (t_g - t_a) = 0.1713 \times 10^{-8} (T_g^4 - T_a^4) \times 0.937 \quad (28)$$

For ordinary glass, $\epsilon = 0.937$ (taken from reference (1) page 162).

For black bodies $\epsilon = 1$

$$h_{c,i} = 0.256 (t_b - t_g)^{0.25} \quad (29)$$

Representing convection transfer between two closely spaced horizontal surfaces.

Internal Radiation:

$$h_{r,i} (t_b - t_g) = 0.1713 \times 10^{-8} (T_b^4 - T_g^4) \times 0.9 \quad (30)$$

0.9 = effective emissivity of the basin bottom and the salt water surface.

$$(H_{a,b} - H_{a,g}) = C_p (t_b - t_g) \quad (31)$$

And from Equation (26), replace $h_{c,i}$ and $(H_{a,b} - H_{a,g})$ by their respective equivalents to get:

$$E = \frac{0.256 (t_b - t_g)^{0.25} (t_b - t_g)}{\frac{W_{da}}{W_{H_2O}} C_p (t_b - t_g)}$$

Thus,

$$E = 0.256 (t_b - t_g)^{0.25} \left(\frac{W_{H_2O}}{W_{da}} \right) 1/C_p \quad (32)$$

Average C_p for air = 0.24 and,

$$E = 0.256 (t_b - t_g)^{0.25} \frac{W_{H_2O}}{0.24 W_{da}} \quad (33)$$

Replace E and other unknowns by their equivalents, in Equations (24) and (25) to get:

$$\begin{aligned} (3.1) (t_g - t_a) + 0.162 \times 10^{-8} (T_g^4 - T_a^4) = \\ 0.256 (t_b - t_g)^{1.25} + 0.156 \times 10^{-8} (T_b^4 - T_g^4) + \\ 1.07 (t_b - t_g)^{0.25} \frac{W_{H_2O}}{W_{da}} \lambda \end{aligned} \quad (34)$$

$$\begin{aligned} \frac{Q_{sh}}{24} = 3.1 (t_g - t_a) + 0.162 \times 10^{-8} (T_g^4 - T_a^4) + \\ 1.07 (t_b - t_g)^{1.25} \left(\frac{W_{H_2O}}{W_{da}} \right) + \frac{50}{24} \end{aligned} \quad (35)$$

Q_{sh} is determined from Weather Bureau Records.

Replace Q_{sh} and t_a by their values in Equations (34) and (35). Equations (34) and (35) are solved by trial and error for the mean t_b and t_g . Substitute t_b and t_g in Equation (26) to find E (rate of distillation).

NOMENCLATURE

Symbol	Definition
A_1	= Area of surface (1) (ft^2).
A_2	= Area of surface (2) (ft^2).
A_3	= Area of surface (3) (ft^2).
A_m	= Logarithmic mean area through which heat flows at right angles (ft^2).
C_p	= Specific heat of stream at constant pressure (Btu/lb- $^{\circ}\text{F}$).
E	= Water evaporation and condensation rate ($\text{lb}/\text{ft}^2\text{-hr}$).
\bar{F}_{12}	= Black surface overall interchange factor, defined as the fraction of the radiation leaving black surface A_1 in all directions which reaches and is absorbed by A_2 , directly and by aid of reflection and/or reradiation.
\mathcal{F}_{13}	= Overall interchange factor, representing the radiation reaching surface A_3 due to original emission from A_1 only, but including assistance given by reflection at other source - sinks.

Symbol	Definition
h'_c	= Convection heat transfer coefficient from the surrounding air to the glass cover (Btu/hr-ft ² -°F).
h	= Local coefficient of heat transfer (Btu/hr-ft ² -°F).
h_c	= Convection heat transfer coefficient from the outside Plexiglas surface to the surrounding atmosphere (Btu/hr-ft ² -°F).
$h_{c,i}$	= Coefficient of convection heat transfer from salt water surface to cover of still (Btu/hr-ft ² -°F).
$h_{c,o}$	= Convection heat transfer coefficient from the glass cover to the atmosphere (Btu/hr-ft ² -°F).
$h_{r,o}$	= Radiation heat transfer coefficient from the glass cover to the atmosphere (Btu/hr-ft ² -°F).
$H_{a,b}$	= Enthalpy of dry air at water basin temperature (Btu/lb).
$H_{a,g}$	= Enthalpy of dry air at cover temperature (Btu/lb).
j	= Dimensionless ordinate.
k	= Thermal conductivity of fluid (Btu/ft-hr-°F).
k_m	= Mean thermal conductivity of the insulation (Btu/hr-ft-°F).
L	= Length of heat transfer surface, heated length, (ft).

Symbol	Definition
q	= Heat loss or gain by conduction (Btu/ft ² -hr).
q'_c	= Net rate of heat transfer by convection from the air to the glass cover (Btu/ft ² -hr).
q'_r	= Net rate of radiation interchange from the air to the glass cover (Btu/ft ² -hr).
q_{ab}	= Rate of heat absorbed by the cover from the incident solar energy (Btu/ft ² -hr).
q_c	= Net rate of convection heat transfer from glass cover to the vapor inside the still (Btu/ft ² -hr).
q_i	= Incident radiation on the glass cover (Btu/ft ² -hr).
q_r	= Net rate of radiation interchange from the glass cover to the water basin (Btu/ft ² -hr).
Q_A	= Rate of heat available for evaporation (Btu/hr).
Q_b	= Rate of heat loss by conduction through the water basin (Btu/hr).
Q_c	= Rate of heat loss by convection from the Plexiglas surface to the surroundings (Btu/hr).
Q_g	= Rate of heat transferred to the vapors passing along the underside of the Plexiglas surface (Btu/hr).

Symbol	Definition
Q_i	= Rate of incident radiation on the Plexiglas cover (Btu/hr-0.785 ft ²).
Q_k	= Rate of heat loss by conduction from the evaporator walls (Btu/hr).
Q_{refl}	= Rate of heat reflected from the outside surface of the Plexiglas cover (Btu/hr).
Q_r	= Net radiation interchange between the Plexiglas cover and the surrounding atmosphere (Btu/hr).
Q_s	= Rate of radiation transmitted through the Plexiglas cover (Btu/hr).
Q_{sh}	= Net solar radiation absorbed on basin bottom, (Btu/ft ²).
	$Q_{sh} =$ incident radiation-(reflection from cover + reflection from salt water surface + reflection from basin bottom) .
Q_t	= (Rate of available heat for evaporation transmitted through the Plexiglas) + (rate of heat gain to the water basin by conduction from the evaporator walls), (Btu/hr).
Q_u	= Rate of heat losses due to vapor absorption by radiation, and other unaccounted for heat losses

Symbol	Definition
	(Btu/hr).
$Q_{1\leftrightarrow 2}$	Net rate of radiation heat interchange between surfaces (1) and (2), (Btu/hr).
$Q_{1\leftrightarrow 3}$	Net rate of radiation heat interchange between surfaces (1) and (3), (btu/hr).
$Q_{3\leftrightarrow 2}$	Net rate of radiation heat interchange between surfaces (3) and (2), (Btu/hr).
Q'	= Rate of heat loss to the walls by convection from the heat transmitted to the inside of the evaporator (Btu/hr).
Q''	= Rate of heat loss by convection from the bare flange (Btu/hr).
t_a	= Temperature of the air surrounding the still ($^{\circ}\text{R.}$).
t_b	= Equilibrium temperature of the water in the basin ($^{\circ}\text{F.}$).
t_g	= Average glass cover temperature ($^{\circ}\text{F.}$).
T_a	= Absolute temperature of the surrounding air ($^{\circ}\text{R.}$).
T_b	= Absolute temperature of the water basin ($^{\circ}\text{R.}$).
T_g	= Average absolute temperature of the glass cover ($^{\circ}\text{R.}$).
T_1	= Absolute temperature of surface (1), ($^{\circ}\text{R.}$).

Symbol	Definition
T_2	= Absolute temperature of surface (2), ($^{\circ}\text{R}.$).
V	= Wind velocity (ft/sec).
V_{∞}	= Approach velocity of stream (ft/hr).
W_{da}	= Rate of dry air circulating inside the still (lb/hr).
W_{H_2O}	= Rate of water distilled (lb/hr).
X	= Dimensionless abscissa.
Greek	
α	= Absorptivity of the Plexiglas cover.
Δt	= Temperature gradient ($^{\circ}\text{F}.$).
Δx	= Insulation thickness (ft).
ϵ	= Emissivity of glass.
λ	= Latent heat of condensation at basin temperature including difference in sensible heat of condensate at basin and cover temperatures, approximately = 1050 (Btu/lb).
μ	= Absolute viscosity of stream at bulk temperature ($\text{lb}_m/\text{ft-hr}$).
σ	= Stefan-Boltzmann constant = 0.1713×10^{-8} ($\text{Btu}/\text{ft}^2\text{-hr-}(\text{^{\circ}\text{R}})^4$).
ρ	= Plexiglas reflectivity.

Symbol	Definition
Greek	
ρ_{∞}	Density of stream of great depth (lb_m/ft^3).
T	Transmissivity of the Plexiglas.